SCISPACE
formerly Typeset

Open access • Posted Content • DOI:10.1101/2021.07.06.451242

Chasing the metabolism of novel syntrophic acetate-oxidizing bacteria in thermophilic methanogenic chemostats — Source link

Zeng Y, Zheng D, Gou M, Xia Yz ...+4 more authors

Institutions: National Institute of Advanced Industrial Science and Technology, Sichuan University, Hong Kong Polytechnic University

Published on: 06 Jul 2021 - bioRxiv (Cold Spring Harbor Laboratory)

Topics: Methanogen, Syntrophy, Energy source and Methanogenesis

Related papers:

- Computational and comparative investigations of syntrophic acetate-oxidising bacteria (SAOB)
- Syntrophic acetate oxidation replaces acetoclastic methanogenesis during thermophilic digestion of biowaste
- Genome recovery and metatranscriptomic confirmation of functional acetate-oxidizing bacteria from enriched anaerobic biogas digesters.
- Genome-Guided Analysis and Whole Transcriptome Profiling of the Mesophilic Syntrophic Acetate Oxidising Bacterium Syntrophaceticus schinkii.
- First Genome Sequence of a Syntrophic Acetate-Oxidizing Bacterium, Tepidanaerobacter acetatoxydans Strain Re1.

Share this paper:

View more about this paper here: https://typeset.io/papers/chasing-the-metabolism-of-novel-syntrophic-acetate-oxidizing-1g6j06x8z6

bioRxiv preprint doi: https://doi.org/10.1101/2021.07.06.451242; this version posted July 6, 2021. The copyright holder for this preprint (which was not certified by peer review) is the author/funder, who has granted bioRxiv a license to display the preprint in perpetuity. It is made available under aCC-BY-NC-ND 4.0 International license.

Chasing the metabolism of novel syntrophic acetate-oxidizing bacteria in thermophilic methanogenic chemostats

Yan Zeng[a], Dan Zheng[b], Min Gou[c], Zi-Yuan Xia[c], Ya-Ting Chen[c,d*], Masaru Konishi Nobu[e,*], Yue-Qin Tang[a,c,*]

[a] Institute of New Energy and Low-carbon Technology, Sichuan University, No. 24, South Section 1, First Ring Road, Chengdu, Sichuan 610065, China

[b] Biogas Institute of Ministry of Agriculture and Rural Affairs, Section 4-13, Renmin Road South, Chengdu 610041, P. R. China

[c] College of Architecture and Environment, Sichuan University, No. 24, South Section 1, First Ring Road, Chengdu, Sichuan 610065, China

[d] Institute for Disaster Management and Reconstruction, Sichuan University–Hong Kong Polytechnic University, Chengdu, Sichuan 610207, China

[e] Bioproduction Research Institute, National Institute of Advanced Industrial Science and Technology (AIST), Central 6, Higashi 1-1-1, Tsukuba, Ibaraki 305-8566, Japan

[*]Correspondence: Ya-Ting Chen, Institute for Disaster Management and Reconstruction, Sichuan University–Hong Kong Polytechnic University, Chengdu, Sichuan 610207, China

and Masaru Konishi Nobu, Bioproduction Research Institute, National Institute of Advanced Industrial Science and Technology (AIST), Central 6, Higashi 1-1-1, Tsukuba, Ibaraki 305-8566, Japan

and Yue-Qin Tang, College of Architecture and Environment, Sichuan University, No. 24, South Section 1, First Ring Road, Chengdu, Sichuan 610065, China

bioRxiv preprint doi: https://doi.org/10.1101/2021.07.06.451242; this version posted July 6, 2021. The copyright holder for this preprint (which was not certified by peer review) is the author/funder, who has granted bioRxiv a license to display the preprint in perpetuity. It is made available under aCC-BY-NC-ND 4.0 International license.

26 Tel. (fax): +86 28 85990936

27 E-mail: cytscu1101@scu.edu.cn and m.nobu@aist.go.jp and tangyq@scu.edu.cn

bioRxiv preprint doi: https://doi.org/10.1101/2021.07.06.451242; this version posted July 6, 2021. The copyright holder for this preprint (which was not certified by peer review) is the author/funder, who has granted bioRxiv a license to display the preprint in perpetuity. It is made available under aCC-BY-NC-ND 4.0 International license.

Abstract

Background: Acetate is the major intermediate of anaerobic digestion of organic waste to CH_4. In anaerobic methanogenic systems, acetate degradation is carried out by either acetoclastic methanogenesis or a syntrophic degradation by a syntrophy of acetate oxidizers and hydrogenotrophic methanogens. Due to challenges in isolation of syntrophic acetate-oxidizing bacteria (SAOB), the diversity and metabolism of SAOB, as well as the mechanisms of their interactions with methanogenic partners remain poorly understood.

Results: In this study, we successfully enriched previously unknown SAOB by operating continuous thermophilic anaerobic chemostats fed with acetate, propionate, butyrate, or isovalerate as the sole carbon and energy source. They represent novel clades belonging to Clostridia, Thermoanaerobacteraceae, Anaerolineae, and Gemmatimonadetes. In these SAOB, acetate is degraded through reverse Wood-Ljungdahl pathway or an alternative pathway mediated by the glycine cleavage system, while the SAOB possessing the latter pathway dominated the bacterial community. Moreover, H_2 is the major product of the acetate degradation by these SAOB, which is mediated by [FeFe]-type electron-confurcating hydrogenases, formate dehydrogenases, and NADPH reoxidation complexes. We also identified the methanogen partner of these SAOB in acetate-fed chemostat, *Methanosarcina thermophila*, which highly expressed genes for CO_2-reducing methanogenesis and hydrogenases to supportively consuming H_2 at transcriptional level. Finally, our bioinformatical analyses further suggested that these previously unknown syntrophic lineages were prevalent and might play critical

bioRxiv preprint doi: https://doi.org/10.1101/2021.07.06.451242; this version posted July 6, 2021. The copyright holder for this preprint (which was not certified by peer review) is the author/funder, who has granted bioRxiv a license to display the preprint in perpetuity. It is made available under aCC-BY-NC-ND 4.0 International license.

roles in thermophilic methanogenic reactors.

Conclusion: This study expands our understanding on the phylogenetic diversity and *in situ* biological functions of uncultured syntrophic acetate degraders, and presents novel insights on how they interact with their methanogens partner. These knowledges strengthen our awareness on the important role of SAO in thermophilic methanogenesis and may be applied to manage microbial community to improve the performance and efficiency of anaerobic digestion.

Keywords: Thermophilic anaerobic digestion, Microbial community, Syntrophic acetate oxidation, Glycine cleavage, Energy conservation

Background

Anaerobic digestion (AD) of organic waste to produce methane offers opportunities to deliver multiple environmental benefits as it encompasses organic waste treatment and renewable energy production. Volatile fatty acids (VFAs) are the main intermediates, and thus syntrophic fatty acid oxidation is thought to be the key step in AD [1]. Notably, acetate serves as the most important intermediate metabolite and the major precursor of methane, accounting for 60 to 80% of methane production in anaerobic digesters [2, 3]. Notably, metabolic disorders would lead to accumulation of acetate in anaerobic digesters, which may cause acidification and reduce methane production, destabilizing the AD systems. Therefore, uncovering the underly mechanism of anaerobic acetate metabolism is fundamental to manage microbial AD system for better performance.

bioRxiv preprint doi: https://doi.org/10.1101/2021.07.06.451242; this version posted July 6, 2021. The copyright holder for this preprint (which was not certified by peer review) is the author/funder, who has granted bioRxiv a license to display the preprint in perpetuity. It is made available under aCC-BY-NC-ND 4.0 International license.

Under methanogenic condition, methane production from acetate follows two routes (i) acetoclastic methanogenesis (Eq. 1), (ii) syntrophic acetate oxidation coupled with hydrogenotrophic methanogenesis (Eqs. 2 and 3) [4].

$$CH_3COO^- + H_2O \rightarrow CH_4 + HCO_3^- \qquad \Delta G^{0'} = -31.0 \text{ kJ mol}^{-1} \qquad (1)$$

$$CH_3COO^- + 4H_2O \rightarrow 2HCO_3^- + 4H_2 + H^+ \qquad \Delta G^{0'} = +104.6 \text{ kJ mol}^{-1} \qquad (2)$$

$$4H_2 + HCO_3^- + H^+ \rightarrow CH_4 + 3H_2O \qquad \Delta G^{0'} = -135.6 \text{ kJ mol}^{-1} \qquad (3)$$

In the former route, acetate is cleaved into carbonyl group and methyl group, then respectively oxidized to CO_2 and reduced to CH_4 by aceticlastic methanogens *Methanosarcina* or *Methanothrix* [5]. In the latter route, both methyl and carbonyl group of acetate are oxidized to CO_2, associated with the generation of H_2. This reaction is thermodynamically unfavorable under standard conditions ($\Delta G^{0'} = +104.6$ kJ mol^{-1}). Thus, "syntrophic" cooperation with hydrogen-scavenging methanogenic partners ($\Delta G^{0'} = -135.6$ kJ mol^{-1}) is necessary to maintain thermodynamic favorability [4, 6]. Previous studies report observation of syntrophic acetate oxidation in selective conditions (*e.g.*, high concentration of ammonia [7], high temperature [8], or low loading rate and long retention time [9]), suggesting that this niche may play an critical role in diverse methanogenic systems that may have challenges in supporting aceticlastic methanogens.

Although six strains of syntrophic acetate-oxidizing bacteria (SAOB) have been cultured, the full diversity and metabolism of SAOB still remain poorly understood. Among described SAOB, while three species (*Thermacetogenium phaeum* [10], *Syntrophaceticus schinkii* [11], and *Tepidanaerobacter acetatoxydans* [12]) possess the

bioRxiv preprint doi: https://doi.org/10.1101/2021.07.06.451242; this version posted July 6, 2021. The copyright holder for this preprint (which was not certified by peer review) is the author/funder, who has granted bioRxiv a license to display the preprint in perpetuity. It is made available under aCC-BY-NC-ND 4.0 International license.

well-known reverse Wood-Ljungdahl (WL) pathway for syntrophic acetate oxidation [13, 14], but two (*Pseudothermotoga lettingae* [15] and *Schunerera ultunensis,* previously *Clostridium ultunense* [16]) lack genes for this classical WL pathway and are suspected to possess an alternative metabolism, potentially mediated by a glycine cleavage system pathway [13, 17]. Moreover, these cultured SAOB are generally detected with low abundances in anaerobic bioreactors [18-21]. Previous studies based on DNA or protein stable isotope probing (SIP) point towards the presence of other phylogenetically distinct uncultured acetate oxidizers in anaerobic digestors [22-24]. Therefore, uncovering the diversity, ecology, metabolism, and symbiotic interactions of these yet-to-be cultured SAOB is essential for improving our understanding and operation of methanogenic bioreactors under stressed conditions.

Furthermore, it is also crucial for understanding the mechanisms of the syntrophic interaction between SAOB and their methanogens partner. Interspecies electron transfer between these two groups is essential to maintain thermodynamic favorability of microbial methanogenesis [25, 26]. Previous survey on syntrophic acetate metabolizers suggested that H_2 has been regarded as electron carrier from acetate oxidizers to methanogens [4, 14, 27]. Several recent studies also suggested that formate transfer also play a role in propionate [28, 29] and isovalerate [30] syntrophic degradation. Direct interspecies electron transfer (DIET) activity has been suggested in enrichment communities degrading propionate and butyrate [31, 32]. However, whether formate transfer and DIET transfer play roles in acetate syntrophic degradation is not yet known.

bioRxiv preprint doi: https://doi.org/10.1101/2021.07.06.451242; this version posted July 6, 2021. The copyright holder for this preprint (which was not certified by peer review) is the author/funder, who has granted bioRxiv a license to display the preprint in perpetuity. It is made available under aCC-BY-NC-ND 4.0 International license.

One effective cultivation-independent approach to studying the physiology and *in situ* metabolism of uncultured organisms is the combination of metagenomics and metatranscriptomics [17, 30, 33, 34]. In this study, we employed such approach to recover genomes (metagenome-assembled genomes, MAGs) and gene expression profiles of novel potential acetate degraders from fatty-acid-fed thermophilic anaerobic chemostats to investigate their catabolic pathways, energy conservation, and metabolic interactions with their methanogens partner.

Results and discussions

Chemostat operation and performance

Eight thermophilic anaerobic chemostats were stably operated with synthetic wastewater containing acetate, propionate, butyrate, or isovalerate as the sole carbon and energy source at different loading rates (Table S1; Materials and Methods). During the steady operation period, the performance of chemostats was stable, *i.e.*, biogas production was stable and concentrations of VFAs in the eight chemostats were markedly low (10~30 mg L^{-1}), indicating that VFAs fed were almost completely degraded by these microbial communities (Table 1 and Fig. S1).

Microbial diversity and community composition of thermophilic anaerobic chemostats

Based on DNA- and RNA-based 16S ribosomal RNA gene analysis, the bacterial community of the thermophilic chemostats contain diverse population belonging to uncultured lineages (Figs. 1 and S2). The dominated bacterial populations included *Firmicutes* (*e.g.*, order MBA03 and family Thermoanaerobacteraceae), *Bacteroidetes*

bioRxiv preprint doi: https://doi.org/10.1101/2021.07.06.451242; this version posted July 6, 2021. The copyright holder for this preprint (which was not certified by peer review) is the author/funder, who has granted bioRxiv a license to display the preprint in perpetuity. It is made available under aCC-BY-NC-ND 4.0 International license.

(Lentimicrobiaceae), and *Chloroflexi* (Anaerolineaceae), which were at high abundance (up to 72%) and activity (up to 41%) in the all the thermophilic chemostats. *Thermodesulfovibrio* displayed low DNA-based relative abundance, but also high activity (up to 18% of transcriptome). Notably, one genus associated with previously isolated syntrophic acetate-oxidizing bacteria (SAOB) (*Tepidanaerobacter*; [12]) was detected but only comprised less than 1% of the total bacterial community.

In regarding to archaeal community, according to 16S rRNA gene analysis, *Methanosarcina* whose relative abundance accounted for 26%~94% and 48%~99% of archaeal community at the DNA and RNA level, respectively, was the active methanogen across all the thermophilic chemostats. *Methanosarcina* OTUs held a 99.5% sequence similarity to multitrophic methanogen *Methanosarcina thermophila* TM-1, which is able to turnout H_2/formate, acetate, methanol to methane [35]. *Methanothermobacter* was dominant in PTL (67%-DNA, 51%-RNA), PTH (47%-DNA, 42%-RNA), and BTL (25%-DNA, 24%-RNA), while *Methanoculleus* predominated in BTH (33%-DNA, 29%-RNA) and VTH (59%-DNA, 9%-RNA) (Fig. S4).

To profile the metabolic capability of such bacteria and methanogens (potential partners and competitors), a total of 173 Gbp metagenomic clean sequences (ATL, 35 Gbp; PTL, 69 Gbp; BTL, 34 Gbp; VTL, 35 Gbp) were obtained. Illumina paired-end reads from the two subsamples (three subsamples in PTL) were co-assembled. Binning the assembled contigs of metagenomes for thermophilic communities yielded 108, 157, 81 and 96 MAGs from ATL, PTL, BTL, and VTL, respectively. To obtain gene expression profiles of the bacteria and archaea in the chemostats, a total of 287 million metatranscriptomic reads (33.6 Gbp, approximately 4.2 Gbp for each RNA sample)

bioRxiv preprint doi: https://doi.org/10.1101/2021.07.06.451242; this version posted July 6, 2021. The copyright holder for this preprint (which was not certified by peer review) is the author/funder, who has granted bioRxiv a license to display the preprint in perpetuity. It is made available under aCC-BY-NC-ND 4.0 International license.

were sequenced and mapped to the MAGs for each chemostat (78–95% of reads mapped using a 100% nucleotide similarity cutoff). Based on mapping metagenomic reads to the obtained MAGs, the bacterial populations retrieved accounted for 79%, 52%, 67% and 67% of the metagenomic reads obtained from ATL, PTL, BTL and VTL (Fig. S3C). In addition, these bacterial populations accounted for 80%, 74%, 65% and 73% of the metatranscriptomic reads from ATL, PTL, BTL and VTL, respectively (Fig. S3D).

As for the methanogen archaea, *Methanosarcina thermophila* (MAG.ATL014) was the active methanogen in ATL, PTL, BTL and VTL, accounting for 18%, 11%, 3% and 15% of the metatranscriptomic reads from PTL, BTL and VTL, respectively (Fig. S5 and Table S2). The activity of hydrogenotrophic methanogens was negligible in ATL. *Methanothermobacter* (MAG.PTL002) was dominant accounting for 13% of the metatranscriptomic reads in PTL. *Methanoculleus* (MAG.BTL076 and MAG.VTL077) predominated in BTL and VTL, accounting for 28% and 8% of the metatranscriptomic reads from BTL and VTL, respectively.

Syntrophic metabolism and energy conservation of acetate-degrading community in ATL

In the analysis of community structure based on 16S rRNA gene sequencing, the relative abundance and RNA-based activity of bacteria was greater than that of archaea in the all the eight chemostats (Fig. S3A and S3B). This phenomenon was also observed in the analysis based on metagenome and metatranscriptome data (Fig. S3C and S3D).

bioRxiv preprint doi: https://doi.org/10.1101/2021.07.06.451242; this version posted July 6, 2021. The copyright holder for this preprint (which was not certified by peer review) is the author/funder, who has granted bioRxiv a license to display the preprint in perpetuity. It is made available under aCC-BY-NC-ND 4.0 International license.

In methanogenic system, syntrophic fatty acid oxidizers convert propionate, butyrate, and isovalerate to acetate and H_2/formate, and symbiotically hand off these by-products to partnering acetate- and H_2-consuming methanogenic archaea [23, 28, 30]. Therefore, it was expected that bacteria displayed high abundance and activity in propionate-, butyrate-, and isovalerate-fed chemostats, which is consistent with our observation. In acetate-fed chemostats, since aceticlastic methanogens, such as *Methanosarcina*, could autonomously degraded acetate, they were expected to dominate the methanogenic communities. However, despite that *Methanosarcina* (99.5% rRNA sequence similarity to *M. thermophila* TM-1; MAG: MAG.ATL014) held a considerably high abundance and activity in our acetate-fed chemostats, the community are unexpectedly dominated by bacterial populations. This result suggested that several bacterial populations may play a significant role in acetate degradation in our acetate-fed chemostats, and potentially be the previously unknown SAOB clades that we were looking for.

High activity of CO_2-reducing methanogenesis in Methanosarcina

Although *Methanosarcina* groups were previously reported as the main competitor of SAOB, since bacterial populations largely dominated the whole community, we hypothesized that *Methanosarcina* groups could also utilize bacteria-produced metabolites (*e.g.*, H_2 and CO_2) to produce methane in our acetate-fed chemostats, playing a role as the partner of the potential SAOB in the community. To test this hypothesis, we first analyzed the metabolic feature of the *Methanosarcina* MAGs in ATL. In accordance with our hypothesis, the dominant *Methanosarcina* MAG.ATL014 interestingly expressed genes for CO_2 reduction (in addition to acetate

bioRxiv preprint doi: https://doi.org/10.1101/2021.07.06.451242; this version posted July 6, 2021. The copyright holder for this preprint (which was not certified by peer review) is the author/funder, who has granted bioRxiv a license to display the preprint in perpetuity. It is made available under aCC-BY-NC-ND 4.0 International license.

209 catabolism; top octile and quartile of expressed genes in the corresponding MAG
210 respectively; Figs. 2 and 3B; Table S3) even though *Methanosarcina* sp. are known to
211 significantly downregulate expression of such genes during acetate degradation as they
212 are not necessary [36, 37]. Decrease in the activity of the CO_2-reducing pathway also
213 results in decreased cellular concentrations (up to 10-fold) of coenzyme F_{420}, an
214 electron carrier for the CO_2 branch during growth on acetate [38], and, though
215 qualitative, *Methanosarcina*-like cells showed higher autofluorescence (at 420 nm) in
216 chemostats where *Methanosarcina* highly expressed the CO_2-reducing pathway (*i.e.*,
217 ATL and ATH compared to PTL in Fig. S6; [28]). Thus, the *Methanosarcina in situ*
218 likely utilizes an alternative electron source in parallel with acetate.

219 Given the lack of exogenous H_2 and methylated compounds (*i.e.*, compounds that
220 would stimulate usage of the CO_2-reducing branch), this may indicate the presence of
221 some bacterial populations in the chemostat catabolizing acetate and syntrophically
222 transferring H_2 and/or electrons to *Methanosarcina*. Supporting this, (i) acetate-
223 degrading *M. thermophila* cells are known to consume H_2 with affinity similar to that
224 of hydrogenotrophic methanogens [39] and (ii) *Methanosarcina* MAG.ATL014 highly
225 expressed hydrogenases (Fig. 3B; Table S4). This is consistent with previous studies
226 that *Methanosarcina* had been observed together with SAOB in acetate-fed
227 thermophilic anaerobic digesters [22, 40]. Moreover, the detection of H_2-utilizing
228 methanogens (*Methanothermobacter* MAG.ATL045 and *Methanomassiliicoccus*
229 MAG.ATL089; albeit at much lower activity levels) also suggests that H_2 transfer is
230 taking place *in situ* (Figs. 2 and 3B; Table S3). The parallel expression of methanol-
231 reducing methanogenesis by *Methanomassiliicoccus* and methyl compound
232 metabolism by *Methanosarcina* suggests that *Methanosarcina* may generate methanol
233 (methanol:coenzyme M methytransferase has been shown to generate methanol *in vitro*

bioRxiv preprint doi: https://doi.org/10.1101/2021.07.06.451242; this version posted July 6, 2021. The copyright holder for this preprint (which was not certified by peer review) is the author/funder, who has granted bioRxiv a license to display the preprint in perpetuity. It is made available under aCC-BY-NC-ND 4.0 International license.

234 *barkeri* [41]) and feed into *Methanomassiliicoccus* methanogenesis.

235

236 ***Putative syntrophic acetate metabolizers***

237 To identify potential uncultured SAOB that may interact with the above
238 methanogens, we performed metabolic reconstruction of the MAGs recovered for
239 abundant and active bacterial populations. Genome- and transcriptome-based
240 prediction of SAOB is challenging given that the conventional acetate oxidation
241 pathway (reverse WL pathway) and the previously proposed glycine-mediated
242 alternative pathway can be used for carbon fixation and serine/glycine biosynthesis
243 respectively. To identify genotypic features associated with SAOB, we performed
244 comparative genomics of isolated SAOB. All isolated SAOB that possess the reverse
245 WL pathway conserve NAD(P) transhydrogenase, while organisms only capable of
246 homoacetogenesis do not encode genes for this enzyme. Both SAOB (*S. ultunensis* and
247 *P. lettingae*) that lack the WL pathway possess NADPH re-oxidizing complexes, albeit
248 different enzymes: NADPH-dependent FeFe hydrogenase (*S. ultunensis*) and NADH-
249 dependent NADP:ferredoxin oxidoreductase (*P. lettingae*). *P. lettingae* has previously
250 been proposed to use a glycine dehydrogenase-mediated pathway for C1 metabolism
251 and *S. ultunensis* may also use this pathway as it lacks the conventional reverse WL
252 pathway. Interestingly, *S. ultunensis* encodes the glycine dehydrogenase directly
253 upstream of NADPH-dependent FeFe hydrogenase, suggesting potential association of
254 glycine metabolism, NADPH reoxidation, and H_2 generation. Thus, we restricted our
255 analysis to populations encoding and highly expressing the WL pathway or glycine-
256 mediated pathway along with NADPH re-oxidation and H_2/formate generation
257 (expression in top quartile of each population's expression profile). To further increase
258 the stringency of our analysis, we further exclude any populations that highly express

bioRxiv preprint doi: https://doi.org/10.1101/2021.07.06.451242; this version posted July 6, 2021. The copyright holder for this preprint (which was not certified by peer review) is the author/funder, who has granted bioRxiv a license to display the preprint in perpetuity. It is made available under aCC-BY-NC-ND 4.0 International license.

amino acid catabolism (which is often NADP-dependent) using expression of glutamate dehydrogenase as a marker (i.e., gdhA/gdhB in top quartile of expression profile).

We identified bacterial populations associated with uncultured Clostridia (MAG.ATL040, MAG.ATL011, MAG.ATL033, and MAG.ATL044), Thermoanaerobacteraceae (MAG.ATL024, MAG.ATL090, and MAG.ATL105), Anaerolineae (MAG.ATL001 and MAG.ATL101) and Gemmatimonadetes (MAG.ATL080) as the potential SAOB that encode the reverse WL and glycine-mediated acetate-oxidizing pathways and complementary NADPH re-oxidation and H_2/formate-generating enzymes (Figs. 2 and S7; Tables S5 and S6) [17, 42]. Phylogenetic analysis revealed that these bacterial populations were distantly related to known SAOB (Fig.4). Furthermore, the Clostridia members (MAG.ATL011, MAG.ATL033, and MAG.ATL044) and Thermoanaerobacteraceae members (MAG.ATL024, MAG.ATL090, and MAG.ATL105) were phylogenetically closely related to each other, but distantly related to any cultured organisms (Fig.4). Based on the above criteria, among these populations, Thermoanaerobacteraceae population (MAG.ATL105), Anaerolineae populations (MAG.ATL001 and MAG.ATL101) and *Clostridia* population (MAG.ATL040) may syntrophically degrade acetate via reverse Wood-Ljungdahl pathway. Thermoanaerobacteraceae population (MAG.ATL024 and MAG.ATL090), *Clostridia* population (MAG.ATL044) and Gemmatimonadetes (MAG.ATL080) may syntrophically degrade acetate via *Thermotogae*-associated pathway; Figs. 2 and 3A; Tables S5 and S6). These results suggested that previously unknown bacterial clades plays a critical role in syntrophic acetate oxidation.

Energy conservation and electron flow in acetate oxidizers

Metabolism under methanogenic conditions necessitates complementation of

bioRxiv preprint doi: https://doi.org/10.1101/2021.07.06.451242; this version posted July 6, 2021. The copyright holder for this preprint (which was not certified by peer review) is the author/funder, who has granted bioRxiv a license to display the preprint in perpetuity. It is made available under aCC-BY-NC-ND 4.0 International license.

284 substrate oxidation with electron balance. Thus, we explored energy conservation
285 systems (*e.g.*, electron transfer and electron confurcation/bifurcation) of the putative
286 acetate oxidizers. Most of the putative SAOB encode cytoplasmic [FeFe]-type electron-
287 confurcating hydrogenases (HydABC) (Figs. 3A and 5; Table S6) that use exergonic
288 oxidation of reduced ferredoxin (Fd_{red}) ($E^{0'}$ = −430 mV) to drive unfavorable H_2
289 generation from NADH oxidation ($E^{0'}$ = −230 mV) [43], a energy conservation strategy
290 associated with syntrophic fatty acid oxidizers [14, 29, 44]. In addition, populations
291 (MAG.ATL080 and MAG.ATL090) performed H_2 generation via the NADPH-
292 dependent [FeFe] hydrogenase (HndABCD) (Figs. 3A and 5; Table S6). The
293 Anaerolineae member (MAG.ATL001) also encodes a cytochrome b-linked NiFe
294 hydrogenase (HybABCO) and a cytosolic NiFe hydrogenase (HoxEFUHY) (Figs. 3A
295 and 5; Table S6). As for formate metabolism, six of eight SAOB MAGs possess a
296 ferredoxin-dependent formate dehydrogenase (FdhH). The Clostridia-related member
297 MAG.ATL044, Thermoanaerobacteraceae (MAG.ATL105), and Anaerolineae
298 (MAG.ATL001) highly expressed a putative NADPH-dependent formate
299 dehydrogenases (FdpAB). MAG.ATL044 harbors a putative NAD^+-dependent
300 electron-bifurcating complex (FdhA-hydBC: formate dehydrogenase organized with
301 HydBC-related subunits) (Figs. 3A and 5; Table S6). Therefore, the putative SAOB
302 identified encode and express enzymes for energy conservation and electron flow that
303 support thermodynamically challenging catabolism and syntrophy.

304 As discussed above, reducing equivalents (*i.e.*, NADH, NADPH and reduced
305 ferredoxin [Fd_{red}]) involve in the actions of hydrogenases and formate dehydrogenases.

bioRxiv preprint doi: https://doi.org/10.1101/2021.07.06.451242; this version posted July 6, 2021. The copyright holder for this preprint (which was not certified by peer review) is the author/funder, who has granted bioRxiv a license to display the preprint in perpetuity. It is made available under aCC-BY-NC-ND 4.0 International license.

Acetate oxidation via reverse WL pathway and glycine-mediated pathway generate both NADH and NADPH, and the latter pathway yields one mol of ATP per mol acetate oxidized (Fig. 2A) [17, 45]. However, Fd_{red} is not directly generated from acetate degradation. To complete acetate degradation, SAOB in acetate-degrading community encode redox complexes supporting electron transfer between (i) NAD(H) and Fd (*Rhodobacter* nitrogen fixation complex Rnf; NADH:Fd oxidoreductase; MAG.ATL080, MAG.ATL024, MAG.ATL044, MAG.ATL090, MAG.ATL105 and MAG.ATL040) [46], (ii) NADP(H) and NAD(H) and Fd (NADH-dependent NADP:Fd oxidoreductase NfnAB; MAG.ATL024, MAG.ATL090, MAG.ATL105, MAG.ATL040, MAG.ATL001 and MAG.ATL101) [17, 43, 47], (iii) NAD(H) and NADP(H) (transhydrogenase PntAB; MAG.ATL080, MAG.ATL024, MAG.ATL044 and MAG.ATL090) [48, 49], (iv) Fd and unknown electron carriers (uncharacterized oxidoreductase Flox:Hdr; MAG.ATL090, MAG.ATL105 and MAG.ATL101) [17, 45, 50] (Figs. 3A and 5; Table S6). Using these complexes, the syntrophic acetate oxidizers may employ reverse electron transport and electron bifurcation to generate H_2.

In addition, we found that MAG.ATL044 contained a more energy-efficient pathway, which might be the reason why it possessed high abundance and activity in ATL (Figs. 3A and 5; Table S6). Analyses of metatranscriptomic indicates that MAG.ATL044 did not express H_2 generation activity, suggesting it converted acetate to formate but not further to H_2 and CO_2 (Figs. 3A and 5; Table S6). This observation is consistent with previous study that some novel acetate-degrading species expressing the glycine-mediated pathway just oxidized acetate to formate (no H_2 generation) in

bioRxiv preprint doi: https://doi.org/10.1101/2021.07.06.451242; this version posted July 6, 2021. The copyright holder for this preprint (which was not certified by peer review) is the author/funder, who has granted bioRxiv a license to display the preprint in perpetuity. It is made available under aCC-BY-NC-ND 4.0 International license.

full-scale anaerobic digesters [51]. Formate was not detected in ATL, indicating that acetate was completely oxidized without accumulation of this metabolic intermediate. In addition, we did not detect F_{420}-reducing formate oxidation (FdhAB) in *Methanosarcina* in ATL. Thus, we suspected other syntrophic species may convert the acetate-derived formate to H_2. In agreement, metagenomics analyses showed that Clostridia (MAG.ATL106) and Anaerolineaceae (MAG.ATL019) highly expressed formate dehydrogenases and hydrogenases (Fig. 5 and Table S6), suggesting potential involvement in formate oxidation [52, 53]. In contrast, another acetate degrader MAG.ATL001, which was the second most active bacterial MAG (accounting for 13.1% of the activity) highly expressed formate dehydrogenases and hydrogenase at similar levels, oxidizing acetate to H_2 and CO_2 via reverse WL pathway (Figs. 3A and 5; Table S6). This result suggests that acetate oxidation by MAG.ATL001 may prefer H_2 for interspecies electron transfer in our thermophilic community. The glycine-mediated pathway avoids endergonic 5-methyl-THF oxidation, generating a yield of 1 ATP per acetate. In comparison, the reverse WL pathway hold a puzzling theoretical yield of 0 ATP per acetate [17] (Fig. 2A). This optimal energy generation strategy might partially explain the high abundance and activity of MAG.ATL044.

In order to improve our understanding of energy conservation revolving around SAO process, we compared electron transfer mechanisms of our novel enriched acetate oxidizers with previously known SAOB. We found a new formate dehydrogenase, FdpAB, located in the novel acetate oxidizers in ATL (Figs. 3A and S8; Tables S6 and S7). *T. phaeum* and *S. schinkii* encode membrane-bound cytochrome b-linked quinone-

bioRxiv preprint doi: https://doi.org/10.1101/2021.07.06.451242; this version posted July 6, 2021. The copyright holder for this preprint (which was not certified by peer review) is the author/funder, who has granted bioRxiv a license to display the preprint in perpetuity. It is made available under aCC-BY-NC-ND 4.0 International license.

dependent formate dehydrogenase (FdnGHI) associated with proton extrusion, which were not found in novel acetate oxidizers in ATL. In addition, all the known groups of formate dehydrogenases were not identified in *T. acetatoxydans* and *P. lettingae*, though they were capable of converting acetate into CO_2 and H_2. These analyses implied potentially high diversity of formate dehydrogenase in SAOB. In terms of hydrogenase, electron-confurcating hydrogenases HydABC has been found in all novel acetate oxidizers and the known SAOB (except *S. ultunense*) (Figs. 3A and S8; Tables S6 and S7), suggesting such electron confurcation mechanism is universal in SAOB. However, several novel acetate oxidizers had depressed expression of HydABC. We speculate that these populations may have unknown hydrogenase and/or they may transfer formate to other syntrophic populations. Morever, Rnf, NfnAB, PntAB and HydABC were well conserved amongst some novel acetate oxidizers and known SAOB, suggesting that they may serve a core function to SAO.

In addition to interspecies electron transfer via hydrogen and formate, DIET has been conceived as a potential mechanism in extracellular electron transfer [54], which depends on electrically conductive type IV pili and outer-surface c-type cytochromes [55]. The putative acetate metabolizers (Only Gemmatimonadetes MAG.ATL080 and Thermoanaerobacteraceae MAG.ATL024) encode a type IV pilin assembly protein (PilC) and a VirB11-like ATPase (PilB), but no genes encoding the structural protein PilA, which is associated with DIET [56], were found (Table S6). A c-type cytochrome was detected in Gemmatimonadetes (MAG.ATL080) and Anaerolineae (MAG.ATL001 and MAG.ATL101), and only MAG.ATL080 and MAG.ATL101 high

bioRxiv preprint doi: https://doi.org/10.1101/2021.07.06.451242; this version posted July 6, 2021. The copyright holder for this preprint (which was not certified by peer review) is the author/funder, who has granted bioRxiv a license to display the preprint in perpetuity. It is made available under aCC-BY-NC-ND 4.0 International license.

372 expressed this gene (Table S6). Therefore, DIET may play a role in syntrophic acetate
373 degradation, but not the essential role. The roles of DIET in these novel acetate
374 degraders remain unclear but warrant further attention.

375 ***Energy-conserving metabolisms in methanogens***

376 In the archaeal community, *Methanosarcina* MAG.ATL014 obtained the electrons
377 from intermediate H_2 through highly expression of methanophenazine(MP)-reducing
378 hydrogenase (VhoGAC), energy-converting [NiFe] hydrogenase (EchA-F), and F_{420}
379 reduction hydrogenase (FrhABG) (Figs. 3B and 5; Table S4). The electrons provided
380 by FrhABG were transferred to F_{420} to produce $F_{420}H_2$. The electrons carried by $F_{420}H_2$
381 were used for two reduction steps (methenyl-H_4MPT→methylene-H_4MPT→methyl-
382 H_4MPT) in hydrogenotrophic methanogenesis, as well as transferred to MP via a FpoF-
383 lacking FpoA-O. Finally, MPH_2 reduced by VhoGAC and FpoA-O transferred
384 electrons to CoM-S-S-CoB via heterodisulphide reductase (HdrDE) (Figs. 3B and 5;
385 Table S4). The metabolism yields energy by forming proton motive force via HdrDE
386 [57, 58]. *Methanosarcina* also highly expressed the heterodisulfide reductase
387 homologous HdrA2B2C2 that oxidize $F_{420}H_2$ with the reduction of Fd_{ox} and CoB-S-S-
388 CoM through flavin-based electron bifurcation [59, 60]. The H_2/CO_2-dependent
389 methanogen *Methanothermobacter* (MAG.ATL045) has genes for H_2 oxidation via
390 reverse electron transport (EhaA-T rather than EchA-F), electron bifurcation
391 (MvhADG-HdrABC), and F_{420} reduction (FrhABG). Nevertheless,
392 *Methanothermobacter* did not express all of above genes for H_2/formate oxidation (Figs.
393 3B and 5; Table S4). *Methanomassiliicoccus* highly expressed genes for electron-

bioRxiv preprint doi: https://doi.org/10.1101/2021.07.06.451242; this version posted July 6, 2021. The copyright holder for this preprint (which was not certified by peer review) is the author/funder, who has granted bioRxiv a license to display the preprint in perpetuity. It is made available under aCC-BY-NC-ND 4.0 International license.

394 bifurcating H_2 oxidation and a putative ferredoxin: heterodisulfide oxidoreductase
395 complex for electron transduction from H_2 to methanol-reducing methanogenesis (via
396 MvhADG, HdrABC, FpoF-lacking Fpo-like, and HdrD) (Fig.3B and 5; Table S4). The
397 high H_2 oxidation activity detected in *Methanosarcina* MAG.ATL014 in ATL was
398 associated with consumption of H_2 produced from SAO and formate oxidation.
399 Moreover, *Methanosarcina* higher expressed the genes involved in CO_2-reducing
400 pathway in ATL compared to PTL and VTL (Tables S3 and S4, [28, 30]). These results
401 implied that *Methanosarcina* played a multi-trophic functional role in thermophilic
402 chemostats.
403
404 **Syntrophic metabolism and energy conservation of acetate-degrading community**
405 **in propionate-, butyrate-, and isovalerate-fed chemostats**
406 As acetate is an important by-product from syntrophic fatty acid degradation (*e.g.*,
407 propionate, butyrate, and isovalerate), SAOB should be also present in the chemostats
408 fed with these fatty acids. To investigate whether the observed novel SAOB in ATL
409 also play roles in oxidation of other fatty acids, we analyzed the metabolic features of
410 the MAGs involved in the microbial communities in other seven chemostats. Similar
411 with the result in ATL, the previously known SAOB (*i.e.*, *T. phaeum*, *P. lettingae*, *S.*
412 *ultunense*, *S. schinkii*, and *T. acetatoxydans*) were not detected in PTL, whereas
413 populations related to the known acetate-oxidizing genus *Tepidanaerobacter*
414 (MAG.BTL055 and MAG.VTL084) only displayed low activity and did not express
415 acetate oxidizing activity in butyrate- and isovalerate-degrading communities (Fig. S7;

bioRxiv preprint doi: https://doi.org/10.1101/2021.07.06.451242; this version posted July 6, 2021. The copyright holder for this preprint (which was not certified by peer review) is the author/funder, who has granted bioRxiv a license to display the preprint in perpetuity. It is made available under aCC-BY-NC-ND 4.0 International license.

Tables S5 and S6). In propionate-, butyrate- and isovalerate-degrading communities, we identified multiple bacterial populations associated with uncultured Clostridia, Thermoanaerobacteraceae, Anaerolineae, Gemmatimonadetes and *Thermodesulfovibrio* that encode the reverse WL and glycine-mediated pathways, associated with complementary NADPH re-oxidation and H_2/formate-generating enzymes (Fig.S7; Tables S5 and S6). Based on the above criteria (See Results and discussion 3.4.1 for details of the settings), among these populations, *Thermodesulfovibrio* (MAG.PTL017 and MAG.VTL073), *Desulfotomaculum* (MAG.BTL007), Thermoanaerobacteraceae populations (MAG.VTL038 and MAG.BTL014), *Clostridia* populations (MAG.PTL141 MAG.BTL065 and MAG.VTL024), and Gemmatimonadetes (MAG.BTL079 and MAG.VTL039) may syntrophically degrade acetate (the former three expressed the reverse Wood-Ljungdahl pathway and the last expressed the *Thermotogae*-associated pathway; Fig.6; Tables S5 and S6). These results confirmed our previous study, in which members of Clostridia, Thermoanaerobacteraceae, Anaerolineae, and *Thermodesulfovibrio* were labeled with $^{13}C_2$-sodium acetate in DNA stable isotope probing assays [23]. Therefore, these microorganisms were potential acetate degrader.

Biosynthetic metabolism of acetate oxidizers

In our chemostats, the novel SAOB used acetate as the carbon and energy source for producing H_2, reducing equivalents (*i.e.*, NADH, NADPH and reduced ferredoxin [Fd_{red}]), and ATP, which provided the cell with energy for biomass biosynthesis. We

bioRxiv preprint doi: https://doi.org/10.1101/2021.07.06.451242; this version posted July 6, 2021. The copyright holder for this preprint (which was not certified by peer review) is the author/funder, who has granted bioRxiv a license to display the preprint in perpetuity. It is made available under aCC-BY-NC-ND 4.0 International license.

438 further found that these novel acetate degraders encode pathways for converting acetyl-
439 CoA to pyruvate, as well as other important precursors for biosynthesis of sugars, amino
440 acids (AAs) and nucleotides, and pathways for AAs degradation (Tables S8-S10).

441 In complex microbial communities, microbes are frequently observed to interact
442 other individuals by exchanging the above mentioned metabolites as public goods [61,
443 62], we thus set out to test whether this is also the case in our novel SAOB. Strikingly,
444 we found that no single SAOB contains all the genes encoding the synthesis of an entire
445 suite of amino acids (AAs) (Fig. S9 and Table S8), suggesting that the exchange of the
446 essential AAs (one typical set of public goods reported previously [63, 64]) is common
447 between these novel SAOB in thermophilic fatty acid-degrading community. Further
448 analyses indicated that acetate degraders tended to lose/ lowly express the AA
449 biosynthetic pathway with higher energy cost (Fig. S9 and Table S8). In addition, the
450 populations which closely related to each other possessed similar capabilities for AA
451 biosynthesis. The Clostridia-related acetate metabolizers (MAG.ATL044,
452 MAG.PTL141, MAG.BTL065 and MAG.VTL024), which displayed the dominant
453 activity in individual chemostat and proposed glycine-mediated acetate oxidation
454 pathway, only synthesized three AAs (*i.e.*, glutamate, glycine, and serine) (Fig. S9 and
455 Table S8). In comparison with the most active acetate degraders (MAG.ATL044,
456 MAG.PTL141, MAG.BTL065 and MAG.VTL024), other acetate degraders have genes
457 for synthesizing more AAs, whereas they had depressed expression of biosynthesis for
458 the majority of AAs (Fig. S9 and Table S8). According to the Black Queen Hypothesis,
459 when an individual loses an energy-expensive function, it becomes a 'beneficiary', who

bioRxiv preprint doi: https://doi.org/10.1101/2021.07.06.451242; this version posted July 6, 2021. The copyright holder for this preprint (which was not certified by peer review) is the author/funder, who has granted bioRxiv a license to display the preprint in perpetuity. It is made available under aCC-BY-NC-ND 4.0 International license.

scavenges the public goods, such as AAs, from other individuals (helpers) for survival [65, 66]. The 'beneficiary' strain will expand in the community until the production of public goods, such as AAs, is just sufficient to support the balanced community. AA biosynthesis is an energy-consuming process, and therefore, the acetate metabolizers can invest more energy to their metabolism on acetate oxidation rather than biosynthesis. These results suggest that the metabolic exchange of public goods between SAOB and other members plays a significant role on maintaining high efficiency of acetate metabolism during the AD process.

The prevalence of the novel SAOB across diverse thermophilic AD communities

The novel acetate degraders from uncultured lineages in this study (members of Clostridia, Thermoanaerobacteraceae, Anaerolineae, and Gemmatimonadetes) from ATL, PTL, BTL and VTL were distantly related to any isolated species (Fig. S10). Moreover, these novel acetate oxidizers were closely related (⩾97% similarity; Fig. S11) to uncultured populations detected in thermophilic anaerobic digesters feeding with a wide diversity of substrates (*e.g.*, sole carbon source [67, 68], binary carbon source [69], municipal waste [70, 71], agricultural waste [72, 73] and industrial waste [74, 75]). Therefore, the novel syntrophic lineages revealed in the present study are the universal and probably core species that play a critical role in thermophilic methanogenic process in thermophilic anaerobic digestion.

Conclusion

bioRxiv preprint doi: https://doi.org/10.1101/2021.07.06.451242; this version posted July 6, 2021. The copyright holder for this preprint (which was not certified by peer review) is the author/funder, who has granted bioRxiv a license to display the preprint in perpetuity. It is made available under aCC-BY-NC-ND 4.0 International license.

In summary, we combined metagenomics and metatrascriptomics to characterize novel syntrophic acetate oxidizers, including Clostridia, Thermoanaerobacteraceae, Anaerolineae, Gemmatimonadetes and *Thermodesulfovibrio* members, in thermophilic anaerobic chemostats. The high expression of genes involved in acetate oxidation and energy conservation systems indicated that these acetate-oxidizing species played an essential role in syntrophic acetate degradation. *Methanosarcina thermophile* highly performed acetate and H_2 utilizing methanogenesis, consuming H_2 derived from acetate oxidizers. These findings improve our understanding of the phylogenetic diversity and metabolic characteristics of the syntrophic acetate oxidizers and their interaction with methanogens, although thoroughly characterization of these newly proposed acetate oxidizers still requires further effortful cultivation-based studies. Managing the performance of these novel bacterial clades may be key to improve the efficiency of anaerobic digestion, facing against serious challenges of the environment degradation and energy shortage.

Materials and Methods

Operation of thermophilic anaerobic chemostats

Eight thermophilic (55 °C) anaerobic chemostats (Fig. S12) were constructed using continuous stirred tank reactors (CSTRs), each with a working volume of 1.8 L. The seed sludge for inoculating acetate- and propionate-degrading chemostats was obtained from a thermophilic anaerobic digester treating kitchen waste (Sichuan Province, China), and the seed sludge for inoculating butyrate- and isovalerate-

bioRxiv preprint doi: https://doi.org/10.1101/2021.07.06.451242; this version posted July 6, 2021. The copyright holder for this preprint (which was not certified by peer review) is the author/funder, who has granted bioRxiv a license to display the preprint in perpetuity. It is made available under aCC-BY-NC-ND 4.0 International license.

degrading chemostats was from a swine manure treatment plant (Sichuan Province, China) (Table S1). The seed sludge was rinsed with the washing solution (synthetic wastewater without carbon sources) thrice under anaerobic condition, diluted to 1.8 L, and then inoculated into each chemostat.

The thermophilic chemostats were fed with synthetic wastewater containing acetate, propionate, butyrate, or isovalerate as the sole carbon source, respectively (total organic carbon [TOC] = 8000 $mg \cdot L^{-1}$) (Table S1). The synthetic wastewater contains 0.3 g/L KH_2PO_4, 4.0 g/L $KHCO_3$, 1.0 g/L NH_4Cl, 0.6 g/L NaCl, 0.82 g/L $MgCl_2 \cdot 6H_2O$, 0.08 g/L $CaCl_2 \cdot 2H_2O$, 0.1 g/L cysteine-$HCl \cdot H_2O$; 10 mL trace element solution containing 21.3 $mg \cdot L^{-1}$ $NiCl_2 \cdot 6H_2O$ and 24.7 $mg \cdot L^{-1}$ $CoCl_2 \cdot 6H_2O$; and 10 mL vitamin solution. 5.46 g sodium acetate and 16.0 g acetic acid were added for acetate synthetic wastewater, 4.27 g sodium propionate and 13.16 g propionic acid were added for propionate synthetic wastewater, 14.67 g butyric acid and 1.33 g NaOH were added for butyrate synthetic wastewater, 13.60 g isovalerate acid and 1.07 g NaOH were added for isovalerate synthetic wastewater.

Briefly, the thermophilic chemostats were incubated in thermostat-controlled water-baths (TR-2A, ASONE, Osaka, Japan). Broth in each chemostat was thoroughly mixed using a magnetic stirrer at 200–300 rpm. Synthetic wastewater was supplied to the chemostats by continuous feeding under an atmosphere of N_2, and the effluent over flowed automatically via a U-type tube. Biogas was collected with a gas holder. Initially, two replicated chemostats were performed for each carbon source, so a total of eight chemostats were operated. The eight thermophilic chemostats were initially operated at

bioRxiv preprint doi: https://doi.org/10.1101/2021.07.06.451242; this version posted July 6, 2021. The copyright holder for this preprint (which was not certified by peer review) is the author/funder, who has granted bioRxiv a license to display the preprint in perpetuity. It is made available under aCC-BY-NC-ND 4.0 International license.

a dilution rate of 0.01 d^{-1} and then increased to 0.025 d^{-1} (hydraulic retention time [HRT] = 40 d), after a period of operation at a dilution rate of 0.025 d^{-1}, dilution rates of four chemostats were increased to 0.05 d^{-1} (hydraulic retention time [HRT] = 20 d). For simplicity, we used A (acetate), P (propionate), B (butyrate), and V (isovalerate) to denote four different carbon sources used in these chemostats; L was used to indicate the lower dilution rate (0.025 d^{-1}), whereas H indicated the higher dilution rate (0.05 d^{-1}). Therefore, the eight chemostats were named as ATL, PTL, BTL, VTL, ATH, PTH, BTH, and VTH, respectively (Table S1).

Broth was sampled every week for fluorescence microscopic observation and physicochemical analyses of pH, suspended solids (SS), volatile suspended solids (VSS), TOC, as well as volatile fatty acids (VFAs) using the same protocols described previously [28]. In addition, the methane and H_2 contents in biogas were determined by a gas chromatograph (GC-2014C, Shimadzu, Kyoto, Japan). During the steady operation period, biomass collected from broth was used for DNA and RNA extraction.

DNA and RNA extraction, 16S rRNA gene PCR, sequencing, and data processing

Sludge was collected from 40 mL broth from each chemostat (ATL, day 286; ATH, day 258; PTL, day 283; PTH, day 400; BTL, day 284; BTH, day 398; VTL, day 300; VTH day 360) by centrifugation at 13000 ×g at 4°C for 10 min. The sludge was rinsed thrice with sterile phosphate buffer saline (PBS) (10 mM, pH 7.5). Total DNA and RNA (duplicates for each sample) were extracted via cyltrimethyl ammonium bromide (CTAB) method [76]. Total RNA was reverse transcribed using PrimeScript™ RT

bioRxiv preprint doi: https://doi.org/10.1101/2021.07.06.451242; this version posted July 6, 2021. The copyright holder for this preprint (which was not certified by peer review) is the author/funder, who has granted bioRxiv a license to display the preprint in perpetuity. It is made available under aCC-BY-NC-ND 4.0 International license.

548 reagent Kit with gDNA Eraser (Perfect Real Time) according to the manufacturer's
549 protocol (Takara, Kusatsu, Japan). DNA and cDNA samples were subjected to 16S
550 rRNA gene amplicon sequencing. The 16S rRNA genes of both bacteria and archaea
551 were amplified through PCR using universal primers 515F (5′-
552 GTGCCAGCMGCCGCGGTAA-3′) and 909R (5′-CCCCGYCAATTCMTTTRAGT-
553 3′) targeting the V4-V5 hypervariable regions. The 16S rRNA gene amplicon
554 sequencing was performed on an Illumina MiSeq platform (Illumina, San Diego, CA,
555 USA) according to the standard protocols by Majorbio Bio-Pharm Technology Co. Ltd.
556 (Shanghai, China). The data processing was conducted using the protocol as previously
557 reported [23].
558
559 **Metagenomic and metatranscriptomic sequencing, as well as the associated**
560 **bioinformatics analyses**
561 Sludge samples for metagenomic sequencing were collected on different dates
562 from ATL (day 306 and 307), PTL (day 223, 293 and 318), BTL (day 251 and 252),
563 VTL (day 295 and 296). Similarly, sludge samples for metatranscriptomic sequencing
564 were collected on two different dates from ATL (day 302 and 305), PTL (day 223, and
565 293), BTL (day 247 and 249), VTL (day 291 and 293). Total DNA and RNA were
566 extracted using CTAB method [76]. Metagenomic DNA was sequenced on an Illumina
567 HiSeq 2000 platform (Illumina). The paired-end reads (2 × 150 bp) were trimmed via
568 Trimmomatic v0.36 [77] with a quality cutoff of 30, sliding window of 6 bp and
569 minimum length cutoff of 100 bp. The clean reads from different metagenomes of the
570 same chemostat were co-assembled via SPAdes v.3.5.0 [78], binned through MetaBAT
571 [79], and checked for completeness and contamination using CheckM [80]. The

bioRxiv preprint doi: https://doi.org/10.1101/2021.07.06.451242; this version posted July 6, 2021. The copyright holder for this preprint (which was not certified by peer review) is the author/funder, who has granted bioRxiv a license to display the preprint in perpetuity. It is made available under aCC-BY-NC-ND 4.0 International license.

572 completeness was calculated based on the number of expected marker genes present in
573 MAGs, while the contamination based on the number of expected marker genes present
574 in multiple copies. Genes were annotated using Prokka [81] and manual curation was
575 performed as described previously [30]. Phylogenomic trees were built with
576 PhyloPhlAn v0.99 ("-u" option) [82], and the tree was edited using iTOL [83].

577 For metatranscriptomics sequencing, total RNA was purified by removing residual
578 DNA by an RNase-free DNase set (Qiagen, Hilden, Germany). Ribosomal RNA was
579 removed from the DNase-treated RNA via the Ribo-Zero rRNA Removal Kits
580 (Illumina). RNAseq libraries were constructed using the TruSeq RNA sample prep kit
581 (Illumina) with the standard protocol. The libraries were sequenced on an Illumina
582 HiSeq2000 sequencer. The paired-end (2 × 150 bp) metatranscriptomic reads were
583 trimmed as DNA-trimming step described above and mapped to MAGs using the
584 BBMap with the parameters as: minid = 1 (v35.85;
585 http://sourceforge.net/projects/bbmap/). The gene expression levels of functional genes
586 from each MAG were calculated as reads per kilobase transcript per million reads
587 mapped to the MAG (RPKM) averaged from duplicate samples. The RPKM was further
588 normalized to the median gene expression level in the heat map illustration for each bin
589 (RPKM-NM) averaged from duplicate samples [33]. Raw sequence data reported in
590 this paper have been deposited (PRJCA005330) in the Genome Sequence Archive in
591 the BIG Data Center, Chinese Academy of Sciences under accession codes CRA004311
592 for 16S rRNA gene, metagenomics and metatranscriptomics sequencing data that are
593 publicly accessible at http://bigd.big.ac.cn/gsa.
594

bioRxiv preprint doi: https://doi.org/10.1101/2021.07.06.451242; this version posted July 6, 2021. The copyright holder for this preprint (which was not certified by peer review) is the author/funder, who has granted bioRxiv a license to display the preprint in perpetuity. It is made available under aCC-BY-NC-ND 4.0 International license.

595

596 ## Acknowledgements

597 This study was funded by the National Natural Science Foundation of China (No.
598 51678378) and the Ministry of Science and Technology of China (No.
599 2016YFE0127700).

600

601 ## References

602 1. Pind PF, Angelidaki I, Ahring BK. Dynamics of the anaerobic process: effects
603 of volatile fatty acids. Biotechnol Bioeng. 2003, 82:791-801.
604 2. Mountfort DO, Asher RA. Changes in proportions of acetate and carbon dioxide
605 used as methane precursors during the anaerobic digestion of bovine waste.
606 Appl Environ Microbiol. 1978, 35:648-54.
607 3. Mackie RI, Bryant MP. Metabolic activity of fatty acid-oxidizing bacteria and
608 the contribution of acetate, propionate, butyrate, and CO_2 to methanogenesis in
609 cattle waste at 40 and 60 ℃. Appl Environ Microbiol. 1981, 41:1363-1373.
610 4. Hattori S. Syntrophic acetate-oxidizing microbes in methanogenic
611 environments. Microbes Environ. 2008, 23:118-27.
612 5. Ferry J. Methane from acetate. J Bacteriol. 1992, 174:5489-5495.
613 6. Kato S, Watanabe K. Ecological and evolutionary interactions in syntrophic
614 methanogenic consortia. Microbes Environ. 2010, 25:145-151.
615 7. Sun L, Müller B, Westerholm M, Schnürer A. Syntrophic acetate oxidation in
616 industrial CSTR biogas digesters. J Biotechnol. 2014, 171:39-44.
617 8. Zhu X, Kougias PG, Treu L, Campanaro S, Angelidaki I. Microbial community

bioRxiv preprint doi: https://doi.org/10.1101/2021.07.06.451242; this version posted July 6, 2021. The copyright holder for this preprint (which was not certified by peer review) is the author/funder, who has granted bioRxiv a license to display the preprint in perpetuity. It is made available under aCC-BY-NC-ND 4.0 International license.

changes in methanogenic granules during the transition from mesophilic to thermophilic conditions. Appl Microbiol Biotechnol. 2017, 101:1313-1322.

9. Shigematsu T, Tang YQ, Kawaguchi H, Ninomiya K, Kijima J, Kobayashi T, Morimura S, Kida K. Effect of dilution rate on structure of a mesophilic acetate-degrading methanogenic community during continuous cultivation. J Biosci Bioeng. 2003, 96:547-558.

10. Hattori S, Kamagata Y, Hanada S, Shoun H. Thermacetogenium phaeum gen. nov., sp. nov., a strictly anaerobic, thermophilic, syntrophic acetate-oxidizing bacterium. Int J Syst Evol Microbiol. 2000, 50:1601-1609.

11. Westerholm M, Roos S, Schnürer A. *Syntrophaceticus schinkii* gen. nov., sp. nov., an anaerobic, syntrophic acetate-oxidizing bacterium isolated from a mesophilic anaerobic filter. FEMS Microbiol Lett. 2010, 309:100-104.

12. Westerholm M, Roos S, Schnürer A. *Tepidanaerobacter acetatoxydans* sp. nov., an anaerobic, syntrophic acetate-oxidizing bacterium isolated from two ammonium-enriched mesophilic methanogenic processes. Syst Appl Microbiol. 2011, 34:260-266.

13. Manzoor S, Bongcam-Rudloff E, Schnürer A, Müller B. Genome-guided analysis and whole transcriptome profiling of the mesophilic syntrophic acetate oxidising bacterium *Syntrophaceticus schinkii*. PLoS One. 2016, 11:e0166520. doi: 10.1371/journal.pone.0166520.

14. Oehler D, Poehlein A, Leimbach A, Müller N, Daniel R, Gottschalk G, Schink B. Genome-guided analysis of physiological and morphological traits of the

bioRxiv preprint doi: https://doi.org/10.1101/2021.07.06.451242; this version posted July 6, 2021. The copyright holder for this preprint (which was not certified by peer review) is the author/funder, who has granted bioRxiv a license to display the preprint in perpetuity. It is made available under aCC-BY-NC-ND 4.0 International license.

640 fermentative acetate oxidizer *Thermacetogenium phaeum*. BMC Genomics.
641 2012, 13:723. doi: 10.1186/1471-2164-13-723.
642 15. Balk M, Weijma J, Stams AJM. *Thermotoga lettingae* sp. nov., a novel
643 thermophilic, methanol-degrading bacterium isolated from a thermophilic
644 anaerobic reactor. Int J Syst Evol Microbiol. 2002, 52:1361-1368.
645 16. Schnurer A, Schink B, Svensson BH. *Clostridium ultunense* sp. nov., a
646 mesophilic bacterium oxidizing acetate in syntrophic association with a
647 hydrogenotrophic methanogenic bacterium. Int J Syst Bacteriol. 1996, 46:1145-
648 1152.
649 17. Nobu MK, Narihiro T, Rinke C, Kamagata Y, Tringe SG, Woyke T, Liu WT.
650 Microbial dark matter ecogenomics reveals complex synergistic networks in a
651 methanogenic bioreactor. ISME J. 2015, 9:1710-1722.
652 18. Ahring BK, Westermann P. Kinetics of butyrate, acetate, and hydrogen
653 metabolism in a thermophilic, anaerobic, butyrate-degrading triculture. Appl
654 Environ Microbiol. 1987, 53:434-439.
655 19. Narihiro T, Terada T, Ohashi A, Kamagata Y, Nakamura K, Sekiguchi Y.
656 Quantitative detection of previously characterized syntrophic bacteria in
657 anaerobic wastewater treatment systems by sequence-specific rRNA cleavage
658 method. Water Res. 2012, 46:2167-2175.
659 20. Treu L, Kougias PG, Campanaro S, Bassani I, Angelidaki I. Deeper insight into
660 the structure of the anaerobic digestion microbial community; the biogas
661 microbiome database is expanded with 157 new genomes. Bioresour Technol.

bioRxiv preprint doi: https://doi.org/10.1101/2021.07.06.451242; this version posted July 6, 2021. The copyright holder for this preprint (which was not certified by peer review) is the author/funder, who has granted bioRxiv a license to display the preprint in perpetuity. It is made available under aCC-BY-NC-ND 4.0 International license.

2016, 216:260-266.

21. Vanwonterghem I, Jensen PD, Rabaey K, Tyson GW. Genome-centric resolution of microbial diversity, metabolism and interactions in anaerobic digestion. Environ Microbiol. 2016, 18:3144-3158.

22. Mosbæk F, Kjeldal H, Mulat DG, Albertsen M, Ward AJ, Feilberg A, Nielsen JL. Identification of syntrophic acetate-oxidizing bacteria in anaerobic digesters by combined protein-based stable isotope probing and metagenomics. ISME J. 2016, 10:2405-18.

23. Zheng D, Wang HZ, Gou M, Nobu MK, Narihiro T, Hu B, Nie Y, Tang YQ. Identification of novel potential acetate-oxidizing bacteria in thermophilic methanogenic chemostats by DNA stable isotope probing. Appl Microbiol Biotechnol. 2019, 103:8631-8645.

24. Ito T, Yoshiguchi K, Ariesyady HD, Okabe S. Identification of a novel acetate-utilizing bacterium belonging to *Synergistes* group 4 in anaerobic digester sludge. ISME J. 2011, 5:1844-1856.

25. Stams AJ, Plugge CM. Electron transfer in syntrophic communities of anaerobic bacteria and archaea. Nat Rev Microbiol. 2009, 7:568-577.

26. Shen L, Zhao Q, Wu X, Li X, Li Q, Wang Y. Interspecies electron transfer in syntrophic methanogenic consortia: from cultures to bioreactors. Renew Sust Energ Rev. 2016, 54:1358-1367.

27. Manzoor S, Schnürer A, Bongcam-Rudloff E, Müller B. Genome-guided analysis of *Clostridium ultunense* and comparative genomics reveal different

bioRxiv preprint doi: https://doi.org/10.1101/2021.07.06.451242; this version posted July 6, 2021. The copyright holder for this preprint (which was not certified by peer review) is the author/funder, who has granted bioRxiv a license to display the preprint in perpetuity. It is made available under aCC-BY-NC-ND 4.0 International license.

684 strategies for acetate oxidation and energy conservation in syntrophic acetate-
685 oxidising bacteria. Genes. 2018, 9.
686 28. Chen YT, Zeng Y, Wang HZ, Zheng D, Kamagata Y, Narihiro T, Nobu MK,
687 Tang YQ. Different interspecies electron transfer patterns during mesophilic and
688 thermophilic syntrophic propionate degradation in chemostats. Microb Ecol.
689 2020, 80:120-132.
690 29. Hidalgo-Ahumada CAP, Nobu MK, Narihiro T, Tamaki H, Liu WT, Kamagata
691 Y, Stams AJM, Imachi H, Sousa DZ. Novel energy conservation strategies and
692 behaviour of Pelotomaculum schinkii driving syntrophic propionate catabolism.
693 Environ Microbiol. 2018, 20:4503-4511.
694 30. Chen YT, Zeng Y, Li J, Zhao XY, Yi Y, Gou M, Kamagata Y, Narihiro T, Nobu
695 MK, Tang YQ. Novel syntrophic isovalerate-degrading bacteria and their
696 energetic cooperation with methanogens in methanogenic chemostats. Environ
697 Sci Technol. 2020. 54(15):9618-9628. doi: 10.1021/acs.est.0c01840.
698 31. Zhao Z, Zhang Y, Yu Q, Dang Y, Li Y, Quan X. Communities stimulated with
699 ethanol to perform direct interspecies electron transfer for syntrophic
700 metabolism of propionate and butyrate. Water Res. 2016, 102:475-484.
701 32. Zhao Z, Li Y, Yu Q, Zhang Y. Ferroferric oxide triggered possible direct
702 interspecies electron transfer between *Syntrophomonas* and *Methanosaeta* to
703 enhance waste activated sludge anaerobic digestion. Bioresour Technol. 2018,
704 250:79-85.
705 33. Nobu MK, Narihiro T, Liu M, Kuroda K, Mei R, Liu WT. Thermodynamically

bioRxiv preprint doi: https://doi.org/10.1101/2021.07.06.451242; this version posted July 6, 2021. The copyright holder for this preprint (which was not certified by peer review) is the author/funder, who has granted bioRxiv a license to display the preprint in perpetuity. It is made available under aCC-BY-NC-ND 4.0 International license.

706 diverse syntrophic aromatic compound catabolism. Environ Microbiol. 2017.
707 19(11): 4576-4586.
708 34. Zhu X, Campanaro S, Treu L, Seshadri R, Ivanova N, Kougias PG, Kyrpides N,
709 Angelidaki I. Metabolic dependencies govern microbial syntrophies during
710 methanogenesis in an anaerobic digestion ecosystem. Microbiome.
711 2020;8(1):22. doi: 10.1186/s40168-019-0780-9.
712 35. Lackner N, Hintersonnleitner A, Wagner AO, Illmer P. Hydrogenotrophic
713 Methanogenesis and Autotrophic Growth of *Methanosarcina thermophila*.
714 Archaea. 2018, 2018:1-7.
715 36. Hovey R, Lentes S, Ehrenreich A, Salmon K, Saba K, Gottschalk G, Gunsalus
716 RP, Deppenmeier U. DNA microarray analysis of *Methanosarcina mazei* Gö1
717 reveals adaptation to different methanogenic substrates. Mol Genet Genomics.
718 2005, 273:225-239.
719 37. Li Q, Li L, Rejtar T, Karger BL, Ferry JG. Proteome of *Methanosarcina*
720 *acetivorans* Part II: comparison of protein levels in acetate- and methanol-
721 grown cells. J Proteome Res. 2005, 4:129-135.
722 38. Heine-Dobbernack E, Schoberth SM, Sahm H. Relationship of intracellular
723 coenzyme F(420) content to growth and metabolic activity of
724 *Methanobacterium bryantii* and *Methanosarcina barkeri*. Appl Environ
725 Microbiol.1988, 54:454-459.
726 39. Ahring BK, Westermann P, Mah RA. Hydrogen inhibition of acetate
727 metabolism and kinetics of hydrogen consumption by *Methanosarcina*

bioRxiv preprint doi: https://doi.org/10.1101/2021.07.06.451242; this version posted July 6, 2021. The copyright holder for this preprint (which was not certified by peer review) is the author/funder, who has granted bioRxiv a license to display the preprint in perpetuity. It is made available under aCC-BY-NC-ND 4.0 International license.

thermophila TM-1. Arch. Microbiol. 1991, 157:38-42.

40. Hao L, Lü F, Mazéas L, Desmond-Le Quéméner E, Madigou C, Guenne A, Shao L, Bouchez T, He P. Stable isotope probing of acetate fed anaerobic batch incubations shows a partial resistance of acetoclastic methanogenesis catalyzed by *Methanosarcina* to sudden increase of ammonia level. Water Res. 2015, 69:90-99.

41. Dong M, Gonzalez TD, Klems MM, Steinberg LM, Chen W, Papoutsakis ET, Bahnson BJ. In vitro methanol production from methyl coenzyme M using the *Methanosarcina barkeri* MtaABC protein complex. Biotechnol Prog. 2017, 33: 1243-1249.

42. Hattori S, Galushko AS, Kamagata Y, Schink B. Operation of the CO dehydrogenase/acetyl coenzyme A pathway in both acetate oxidation and acetate formation by the syntrophically acetate-oxidizing bacterium *Thermacetogenium phaeum*. J Bacteriol. 2005, 187:3471-6.

43. Buckel W, Thauer RK. Energy conservation via electron bifurcating ferredoxin reduction and proton/Na(+) translocating ferredoxin oxidation. Biochim Biophys Acta. 2013, 1827:94-113.

44. McInerney MJ, Rohlin L, Mouttaki H, Kim U, Krupp RS, Rios-Hernandez L, Sieber J, Struchtemeyer CG, Bhattacharyya A, Campbell JW, Gunsalus RP. The genome of *Syntrophus aciditrophicus*: life at the thermodynamic limit of microbial growth. Proc Natl Acad Sci U S A. 2007, 104:7600-7605.

45. Sieber JR, McInerney MJ, Gunsalus RP. Genomic insights into syntrophy: the

bioRxiv preprint doi: https://doi.org/10.1101/2021.07.06.451242; this version posted July 6, 2021. The copyright holder for this preprint (which was not certified by peer review) is the author/funder, who has granted bioRxiv a license to display the preprint in perpetuity. It is made available under aCC-BY-NC-ND 4.0 International license.

paradigm for anaerobic metabolic cooperation. Annu Rev Microbiol. 2012, 66:429-52.

46. Biegel E, Schmidt S, González JM, Müller V. Biochemistry, evolution and physiological function of the Rnf complex, a novel ion-motive electron transport complex in prokaryotes. Cell Mol Life Sci. 2010, 68:613-634.

47. Wang S, Huang H, Moll J, Thauer RK. $NADP^+$ reduction with reduced ferredoxin and $NADP^+$ reduction with NADH are coupled via an electron-bifurcating enzyme complex in *Clostridium kluyveri*. J Bacteriol. 2010, 192:5115-23.

48. Sauer U, Canonaco F, Heri S, Perrenoud A, Fischer E. The soluble and membrane-bound transhydrogenases UdhA and PntAB have divergent functions in NADPH metabolism of Escherichia coli. J Biol Chem. 2004, 279:6613-9.

49. Shi A, Zhu X, Lu J, Zhang X, Ma Y. Activating transhydrogenase and NAD kinase in combination for improving isobutanol production. Metab Eng. 2013, 16:1-10.

50. Nobu MK, Narihiro T, Hideyuki T, Qiu YL, Sekiguchi Y, Woyke T, Goodwin L, Davenport KW, Kamagata Y, Liu WT. The genome of *Syntrophorhabdus aromaticivorans* strain UI provides new insights for syntrophic aromatic compound metabolism and electron flow. Environ Microbiol. 2015. 17(12):4861-72. doi: 10.1111/1462-2920.12444.

51. Nobu MK, Narihiro T, Mei R, Kamagata Y, Lee PKH, Lee PH, McInerney MJ,

bioRxiv preprint doi: https://doi.org/10.1101/2021.07.06.451242; this version posted July 6, 2021. The copyright holder for this preprint (which was not certified by peer review) is the author/funder, who has granted bioRxiv a license to display the preprint in perpetuity. It is made available under aCC-BY-NC-ND 4.0 International license.

772 Liu WT. Catabolism and interactions of uncultured organisms shaped by eco-
773 thermodynamics in methanogenic bioprocesses. Microbiome. 2020. 8(1): 111.
774 doi: 10.1186/s40168-020-00885-y.
775 52. Dolfing J, Jiang B, Henstra AM, Stams AJ, Plugge CM. Syntrophic growth on
776 formate: a new microbial niche in anoxic environments. Appl Environ
777 Microbiol. 2008, 74:6126-6131.
778 53. Lv XM, Yang M, Dai LR, Tu B, Chang C, Huang Y, Deng Y, Lawson PA, Zhang
779 H, Cheng L, Tang YQ. *Zhaonella formicivorans* gen. nov., sp. nov., an anaerobic
780 formate-utilizing bacterium isolated from Shengli oilfield, and proposal of four
781 novel families and Moorellales ord. nov. in the phylum Firmicutes. Int J Syst
782 Evol Microbiol. 2020, 70:3361-3373.
783 54. Reguera G, McCarthy KD, Mehta T, Nicoll JS, Tuominen MT, Lovley DR.
784 Extracellular electron transfer via microbial nanowires. Nature. 2005, 435:p.
785 1098-1101.
786 55. Malvankar NS, Lovley DR. Microbial nanowires for bioenergy applications.
787 Curr Opin Biotechnol. 2014, 27:88-95.
788 56. Walker DJF, Nevin KP, Holmes DE, Rotaru AE, Ward JE, Woodard TL, Zhu J,
789 Ueki T, Nonnenmann SS, McInerney MJ, Lovley DR. *Syntrophus* conductive
790 pili demonstrate that common hydrogen-donating syntrophs can have a direct
791 electron transfer option. ISME J. 2020, 14:837-846.
792 57. Welte C, Krätzer C, Deppenmeier U. Involvement of Ech hydrogenase in energy
793 conservation of *Methanosarcina mazei*. FEBS J. 2010, 277:3396-3403.

bioRxiv preprint doi: https://doi.org/10.1101/2021.07.06.451242; this version posted July 6, 2021. The copyright holder for this preprint (which was not certified by peer review) is the author/funder, who has granted bioRxiv a license to display the preprint in perpetuity. It is made available under aCC-BY-NC-ND 4.0 International license.

794 58. Welte C, Deppenmeier U. Bioenergetics and anaerobic respiratory chains of
795 aceticlastic methanogens. Biochim Biophys Acta. 2014, 1837:1130-1147.
796 59. Yan Z, Wang M, Ferry JG. A Ferredoxin- and $F_{420}H_2$-dependent, electron-
797 bifurcating, heterodisulfide reductase with homologs in the domains bacteria
798 and archaea. mBio. 2017. 8(1): e02285-16. doi: 10.1128/mBio.02285-16.
799 60. Holmes DE, Rotaru AE, Ueki T, Shrestha PM, Ferry JG, Lovley DR. Electron
800 and proton flux for carbon dioxide reduction in *Methanosarcina barkeri* during
801 direct interspecies electron transfer. Front Microbiol. 2018. 9: 3109. doi:
802 10.3389/fmicb.2018.03109.
803 61. West SA, Griffin AS, Gardner A, Diggle SP. Social evolution theory for
804 microorganisms. Nat Rev Microbiol. 2006, 4:597-607.
805 62. Liu Y-F, Galzerani DD, Mbadinga SM, Zaramela LS, Gu J-D, Mu B-Z, Zengler
806 K. Metabolic capability and in situ activity of microorganisms in an oil reservoir.
807 Microbiome. 2018 Jan 5;6(1):5. doi: 10.1186/s40168-017-0392-1.
808 63. Mee MT, Collins JJ, Church GM, Wang HH. Syntrophic exchange in synthetic
809 microbial communities. Proc Natl Acad Sci U S A. 2014, 111:E2149-E2156.
810 64. Zomorrodi AR, Segrè D. Genome-driven evolutionary game theory helps
811 understand the rise of metabolic interdependencies in microbial communities.
812 Nat Commun. 2017, 8:1563. doi: 10.1038/s41467-017-01407-5.
813 65. Morris JJ, Lenski RE, Zinser ER. The Black Queen Hypothesis: evolution of
814 dependencies through adaptive gene loss. mBio. 2012, 3:e00036-12. doi:
815 10.1128/mBio.00036-12.

bioRxiv preprint doi: https://doi.org/10.1101/2021.07.06.451242; this version posted July 6, 2021. The copyright holder for this preprint (which was not certified by peer review) is the author/funder, who has granted bioRxiv a license to display the preprint in perpetuity. It is made available under aCC-BY-NC-ND 4.0 International license.

816 66. Wang M, Liu X, Nie Y, Wu XL. Selfishness driving reductive evolution shapes
817 interdependent patterns in spatially structured microbial communities. ISME J.
818 2020. doi: 10.1038/s41396-020-00858-x.
819 67. Tang YQ, Matsui T, Morimura S, Wu XL, Kida K. Effect of temperature on
820 microbial community of a glucose-degrading methanogenic consortium under
821 hyperthermophilic chemostat cultivation. J Biosci Bioeng. 2008, 106:180-187.
822 68. Cheng L, He Q, Ding C, Dai LR, Li Q, Zhang H. Novel bacterial groups
823 dominate in a thermophilic methanogenic hexadecane-degrading consortium.
824 FEMS Microbiol Ecol. 2013, 85:568-577.
825 69. Ueno, Y. and Tatara, M. Microbial population in a thermophilic packed-bed
826 reactor for methanogenesis from volatile fatty acids. Enzyme and Microbial
827 Technology. 2008, 43:302-308.
828 70. Tang YQ, Shigematsu T, Ikbal, Morimura S, Kida K. The effects of micro-
829 aeration on the phylogenetic diversity of microorganisms in a thermophilic
830 anaerobic municipal solid-waste digester. Water Res. 2004, 38:2537-2550.
831 71. Goberna M, Insam H, Franke-Whittle IH. Effect of biowaste sludge maturation
832 on the diversity of thermophilic bacteria and archaea in an anaerobic reactor.
833 Appl Environ Microbiol. 2009, 75:2566-2572.
834 72. Weiss A, Jérôme V, Burghardt D, Likke L, Peiffer S, Hofstetter EM, Gabler R,
835 Freitag R. Investigation of factors influencing biogas production in a large-scale
836 thermophilic municipal biogas plant. Appl Microbiol Biotechnol. 2009, 84:987-
837 1001.

bioRxiv preprint doi: https://doi.org/10.1101/2021.07.06.451242; this version posted July 6, 2021. The copyright holder for this preprint (which was not certified by peer review) is the author/funder, who has granted bioRxiv a license to display the preprint in perpetuity. It is made available under aCC-BY-NC-ND 4.0 International license.

838 73. Lachnit T, Meske D, Wahl M, Harder T, Schmitz R. Epibacterial community
839 patterns on marine macroalgae are host-specific but temporally variable.
840 Environ Microbiol. 2011, 13:655-665.
841 74. Wang TT, Sun ZY, Huang YL, Tan L, Tang YQ, Kida K. Biogas production from
842 distilled grain waste by thermophilic dry anaerobic digestion: pretreatment of
843 feedstock and dynamics of microbial community. Appl Biochem Biotechnol.
844 2018, 184:685-702.
845 75. Hillion ML, Moscoviz R, Trably E, Leblanc Y, Bernet N, Torrijos M, Escudié
846 R. Co-ensiling as a new technique for long-term storage of agro-industrial waste
847 with low sugar content prior to anaerobic digestion. Waste Manag. 2018,
848 71:147-155.
849 76. Griffiths RI, Whiteley AS, O'Donnell AG, Bailey MJ. Rapid method for
850 coextraction of DNA and RNA from natural environments for analysis of
851 ribosomal DNA- and rRNA-based microbial community composition. Appl
852 Environ Microbiol. 2000, 66:5488-5491.
853 77. Bolger AM, Lohse M, Usadel B. Trimmomatic: a flexible trimmer for Illumina
854 sequence data. Bioinformatics. 2014, 30:2114-2120.
855 78. Bankevich A, Nurk S, Antipov D, Gurevich AA, Dvorkin M, Kulikov AS, Lesin
856 VM, Nikolenko SI, Pham S, Prjibelski AD, Pyshkin AV, Sirotkin AV, Vyahhi N,
857 Tesler G, Alekseyev MA, Pevzner PA. SPAdes: a new genome assembly
858 algorithm and its applications to single-cell sequencing. J Comput Biol. 2012,
859 19:455-477.

bioRxiv preprint doi: https://doi.org/10.1101/2021.07.06.451242; this version posted July 6, 2021. The copyright holder for this preprint (which was not certified by peer review) is the author/funder, who has granted bioRxiv a license to display the preprint in perpetuity. It is made available under aCC-BY-NC-ND 4.0 International license.

79. Kang DD, Froula J, Egan R, Wang Z. MetaBAT, an efficient tool for accurately reconstructing single genomes from complex microbial communities. PeerJ. 2015, 3:e1165.

80. Parks DH, Imelfort M, Skennerton CT, Hugenholtz P, Tyson GW. CheckM: assessing the quality of microbial genomes recovered from isolates, single cells, and metagenomes. Genome Res. 2015, 25:1043-1055.

81. Torsten S: Prokka: rapid prokaryotic genome annotation. *Bioinformatics* 2014, 30:2068-2069.

82. Segata N, Börnigen D, Morgan XC, Huttenhower C. PhyloPhlAn is a new method for improved phylogenetic and taxonomic placement of microbes. Nat Commun. 2013, 4:2304-2304.

83. Letunic I, Bork P. Interactive tree of life (iTOL) v3: an online tool for the display and annotation of phylogenetic and other trees. Nucleic Acids Res. 2016, 44:W242-245.

Table 1. Operational performance of mesophilic and thermophilic chemostats during the steady operation period [a].

Chemostat name	ATL	ATH	PTL	PTH	BTL	BTH	VTL	VTH
Carbon source	Acetate	Acetate	Propionate	Propionate	Butyrate	Butyrate	Isovalerate	Isovalerate
Dilution rate (day^{-1})	0.025	0.05	0.025	0.05	0.025	0.05	0.025	0.05
HRT (day)	40	20	40	20	40	20	40	20
Inflow concentration ($mg \cdot L^{-1}$)	20000	20000	16444	16444	14667	14667	13600	13600
Gas production rate ($mL \cdot L^{-1} \cdot d^{-1}$)	115±22	294±67	103±17	383±43	155±28	396±35	143±37	365±18
CH_4 content (%)	58±4	60±5	62±2	63±3	66±2	73±4	67±4	76±6
H_2 partial pressure (Pa)	0.8±0.4	1.4±0.6	2.9±1.2	3.1±1.3	2.3±1.4	2.9±1.3	2.0±1.2	2.5±0.9
pH	8.04±0.14	7.85±0.14	7.95±0.14	7.78±0.14	7.78±0.08	7.63±0.11	7.84±0.14	7.66±0.10
TOC ($mg \cdot L^{-1}$)	139±83	132±78	84±49	118±46	87±74	123±91	84±49	114±44
Formate ($mg \cdot L^{-1}$)[b]	ND	ND	ND	ND	ND	ND	ND	ND
Acetate ($mg \cdot L^{-1}$)	11±22	12±35	6±8	2±4	31±47	27±69	23±53	20±20
Propionate ($mg \cdot L^{-1}$)	0	0	11±13	15±48	~1.0	~1.0	~1.0	~1.0
Butyrate ($mg \cdot L^{-1}$)	0	0	0	0	~1.0	~1.0	~1.0	~1.0
Valerate ($mg \cdot L^{-1}$)	0	0	0	0	0	0	~1.0	~1.0
Iso-valerate ($mg \cdot L^{-1}$)	0	0	0	0	0	0	~1.0	~1.0
SS ($g \cdot L^{-1}$)	0.421±0.08	0.543±0.14	0.468±0.11	0.68±0.07	1.43±0.49	1.44±0.38	1.35±0.44	1.38±0.25
VSS ($g \cdot L^{-1}$)	0.308±0.07	0.392±0.11	0.352±0.10	0.513±0.07	0.62±0.21	0.65±0.18	0.57±0.21	0.67±0.19

[a] HRT, hydraulic retention time; TOC, total organic carbon; VSS, volatile suspended solid; ND, not detected. The operational parameters (*e.g.*, pH, gas production rate, and CH_4 content, etc.) were the averages (mean ± SD, n > 30) during the steady-state period in ATL (day 100–550), ATH (day 80–550), PTL (day 100–650), PTH (day 300–450), BTL (day 100–650), BTH (day 300–650), VTL (day 150–650), AND ATL (day 300–650) chemostats (Fig. S2). [b] Formate concentration was below the detective limit (10 mg L^{-1}) of the high-performance liquid chromatography.

bioRxiv preprint doi: https://doi.org/10.1101/2021.07.06.451242; this version posted July 6, 2021. The copyright holder for this preprint (which was not certified by peer review) is the author/funder, who has granted bioRxiv a license to display the preprint in perpetuity. It is made available under aCC-BY-NC-ND 4.0 International license.

879 **Figure Legends**

880 **Fig. 1.** Relative abundance of bacterial genera based on 16S rRNA gene amplicon
881 sequencing in the thermophilic chemostats (DNA level).

882 **Fig. 2.** Metabolic pathways of acetate oxidation and methanogenesis in thermophilic
883 acetate-degrading chemostat (A), and distribution of catabolic pathways among the
884 studied contributors (B). For each syntroph and methanogen, we show presence
885 (indicated by filled circle) of genes encoding pathways for acetate catabolism and
886 methanogenesis. Enzyme abbreviations are as follows: Ack, acetate kinase; Pta,
887 phosphate acetyltransferase; Acs, acetyl-CoA synthetase; CODH complex, acetyl CoA
888 synthetase complex; AcsE, methyltetrahydrofolate:corrinoid/iron-sulfur protein
889 methyltransferase; MetF, methylenetetrahydrofolate reductase; FolD,
890 methylenetetrahydrofolate dehydrogenase/cyclohydrolase; Fhs, formate--
891 tetrahydrofolate ligase; Fdh, formate dehydrogenase. Grd, glycine reductase; Por,
892 pyruvate dehydrogenase; PflD, pyruvate-formate lyase; Sda, serine dehydratase; GlyA,
893 glycine hydroxymethyltransferase; GcvPA, glycine dehydrogenase subunit A; GcvPB**,**
894 glycine dehydrogenase subunit B, GcvT, glycine cleavage system T protein; GcvH,
895 glycine cleavage system H protein; Dld, dihydrolipoyl dehydrogenase. Fmd,
896 formylmethanofuran dehydrogenase; Ftr, formylmethanofuran-
897 tetrahydromethanopterin N-formyltransferase; Mch, methenyltetrahydromethanopterin
898 cyclohydrolase; Mtd, methylenetetrahydromethanopterin dehydrogenase; Mer, F_{420}-
899 dependent 5,10-methenyltetrahydromethanopterisn reductase; Cdh, acetyl-CoA
900 decarbonylase/synthase complex; Mta, [methyl-Co(III) methanol-specificcorrinoid
901 protein]:CoM methyltransferase; Mtb, [methyl-Co(III) dimethylamine-
902 specificcorrinoid protein]:CoM methyltransferase; Mtm, [methyl-Co(III)
903 monomethylamine-specificcorrinoid protein]:CoM methyltransferase ; Mtr,
904 tetrahydromethanopterin S-methyltransferase; Mcr, methyl-CoM reductase. CHO-
905 MF, formyl-methanofuran; CHO-H_4MPT, formyl-tetrahydromethanopterin;
906 CH≡H_4MPT, methenyl-tetrahydromethanopterin; CH_2=H_4MPT, methylene-
907 tetrahydromethanopterin; CH_3-H_4MPT, methyl-tetrahydromethanopterin; CH_3-S-CoM,
908 methyl-coenzyme M; HS-CoM, coenzyme M; HS-CoB, coenzyme B; CoB-S-S-CoM,
909 mixed disulphide of CoM and CoB. Enzyme abbreviations and their corresponding
910 genes are elaborated in Supporting Information Tables S3 and S5.

911 **Fig. 3.** Gene expression level for acetate oxidation, H_2/formate metabolism, and
912 electron transfer genes in syntrophs which may syntrophically degrade acetate (A)

bioRxiv preprint doi: https://doi.org/10.1101/2021.07.06.451242; this version posted July 6, 2021. The copyright holder for this preprint (which was not certified by peer review) is the author/funder, who has granted bioRxiv a license to display the preprint in perpetuity. It is made available under aCC-BY-NC-ND 4.0 International license.

and methanogens (B) from thermophilic acetate-degrading chemostat. For each metagenome-assembled genome (MAG), the percentages of the metatranscriptomic (MT) reads mapped to the MAG out of the metatranscriptomics mapped to all MAGs (both *Bacteria* and *Archaea*) are shown. The gene expression levels are calculated as reads per kilobase of transcript per million reads mapped to individual MAG (RPKM) normalized to the median gene expression for the corresponding MAG (RPKM-NM) averaged from duplicate samples. Pathways containing genes with RPKM-NM greater than the octile and quartile are marked (filled and open dots, respectively). Enzyme abbreviations and their corresponding genes are elaborated in Supporting Information Tables S3-S6.

Fig. 4. Phylogenetic analyses of metagenome-assembled genomes (MAGs) of syntrophs in thermophilic acetate-degrading chemostat. The corresponding abundance of MAGs are estimated from their metagenomic coverage calculated as the percentage of metagenomics (MG) reads mapped to each MAG relative to the total reads mapped to all bacterial and archaeal MAGs. The estimated activity of MAGs in acetate-degrading chemostat are shown as the percentage of metatranscriptomic (MT) reads mapped to each MAG relative to total reads mapped to all bacterial and archaeal MAGs (T, totoal MT reads; T1, MT reads of sampling time point 1; T2, MT reads of sampling time point 2).

Fig. 5. Overview of the metabolism of syntrophs and methanogens from thermophilic acetate-degrading communities. Hydrogenase, formate dehydrogenases and energy conservation pathways are abbreviated as shown in Supporting Information Tables S3-S6.

Fig. 6. Gene expression level for acetate oxidation, H_2/formate metabolism, and electron transfer genes in syntrophs which may syntrophically degrade acetate from thermophilic chemostats. For each MAG, the percentages of the metatranscriptomic (MT) reads mapped to the MAG out of the metatranscriptomics mapped to all MAGs (both *Bacteria* and *Archaea*) are shown. The gene expression levels are calculated as reads per kilobase of transcript per million reads mapped to individual MAG (RPKM) normalized to the median gene expression for the corresponding MAG (RPKM-NM) averaged from duplicate samples. Pathways containing genes with RPKM-NM greater than the octile and quartile are marked (filled and open dots, respectively). Enzyme abbreviations and their corresponding genes are elaborated in Supporting Information Tables S5-S6.

bioRxiv preprint doi: https://doi.org/10.1101/2021.07.06.451242; this version posted July 6, 2021. The copyright holder for this preprint (which was not certified by peer review) is the author/funder, who has granted bioRxiv a license to display the preprint in perpetuity. It is made available under aCC-BY-NC-ND 4.0 International license.

947 **Fig. 1.**

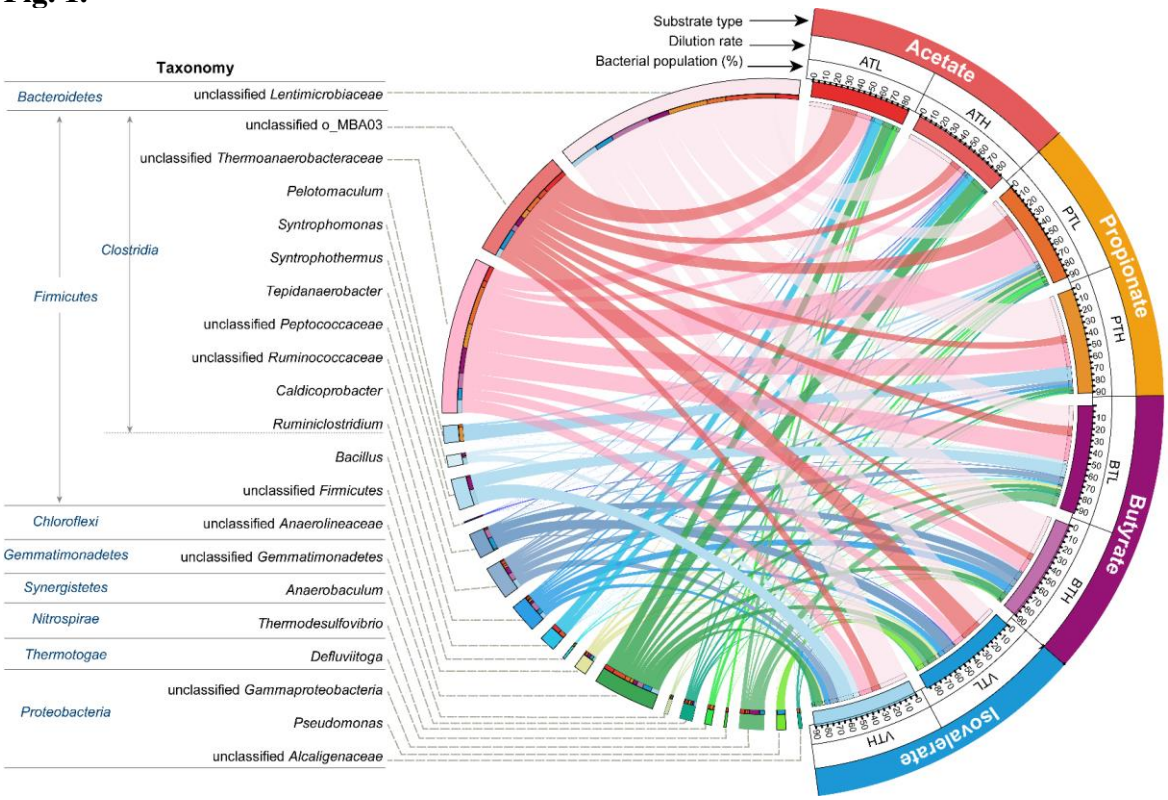

948

bioRxiv preprint doi: https://doi.org/10.1101/2021.07.06.451242; this version posted July 6, 2021. The copyright holder for this preprint (which was not certified by peer review) is the author/funder, who has granted bioRxiv a license to display the preprint in perpetuity. It is made available under aCC-BY-NC-ND 4.0 International license.

949 **Fig. 2.**

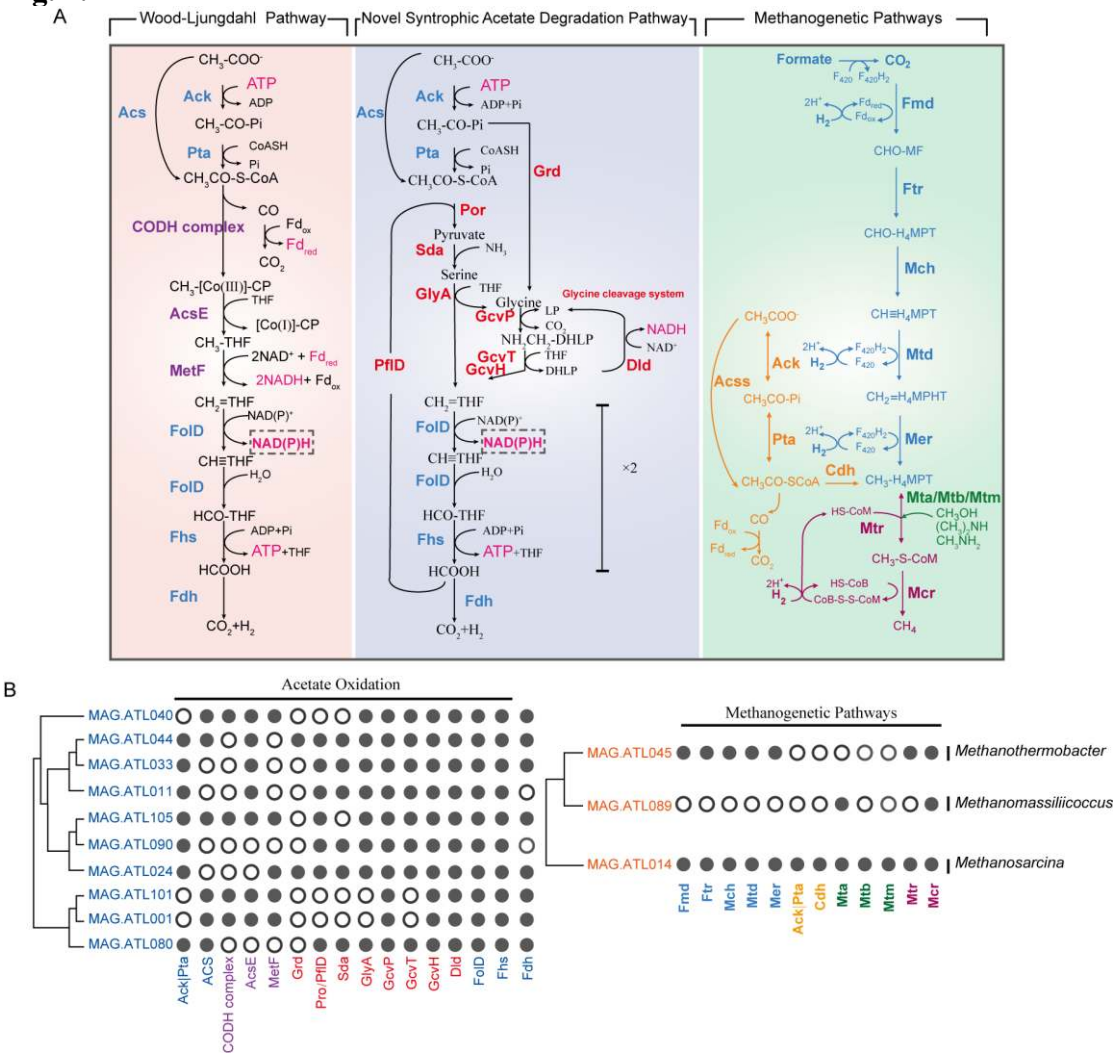

950

bioRxiv preprint doi: https://doi.org/10.1101/2021.07.06.451242; this version posted July 6, 2021. The copyright holder for this preprint (which was not certified by peer review) is the author/funder, who has granted bioRxiv a license to display the preprint in perpetuity. It is made available under aCC-BY-NC-ND 4.0 International license.

951 **Fig. 3.**

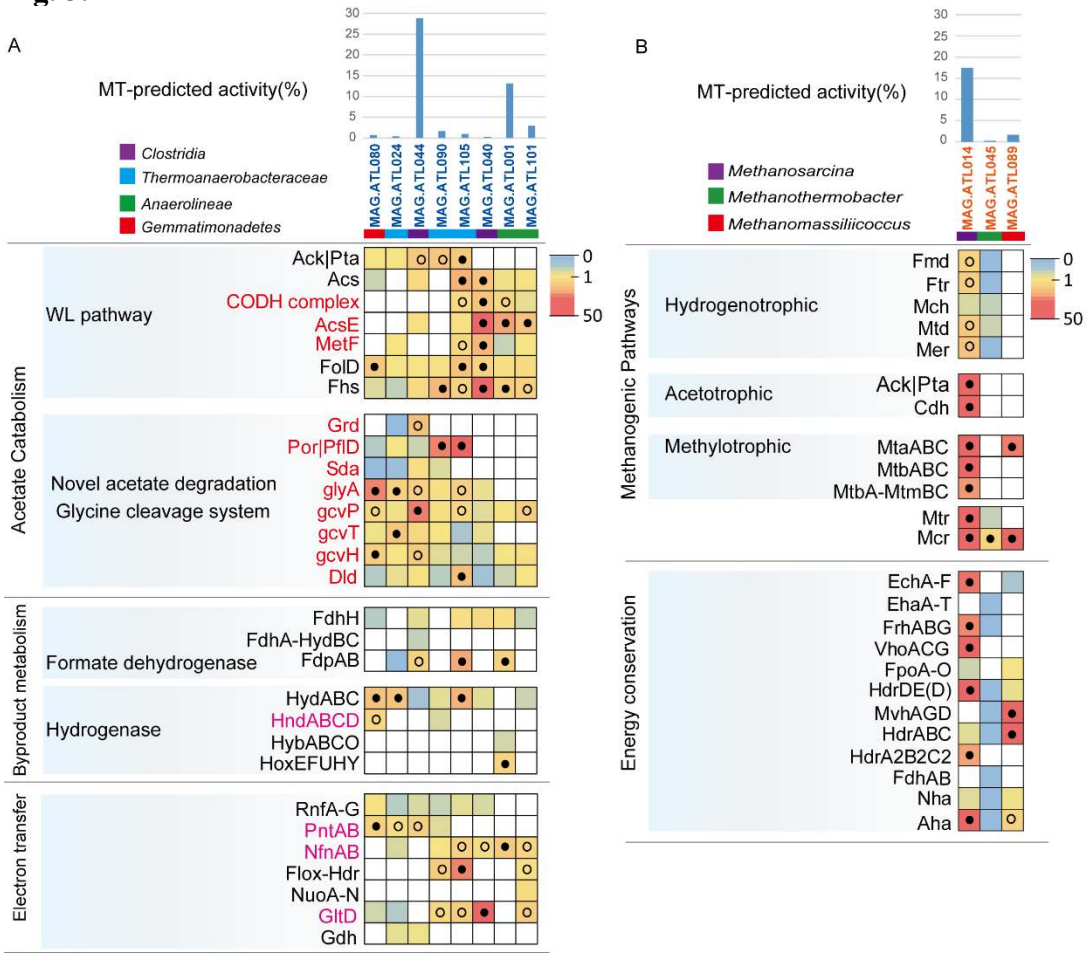

952

bioRxiv preprint doi: https://doi.org/10.1101/2021.07.06.451242; this version posted July 6, 2021. The copyright holder for this preprint (which was not certified by peer review) is the author/funder, who has granted bioRxiv a license to display the preprint in perpetuity. It is made available under aCC-BY-NC-ND 4.0 International license.

953 **Fig. 4.**

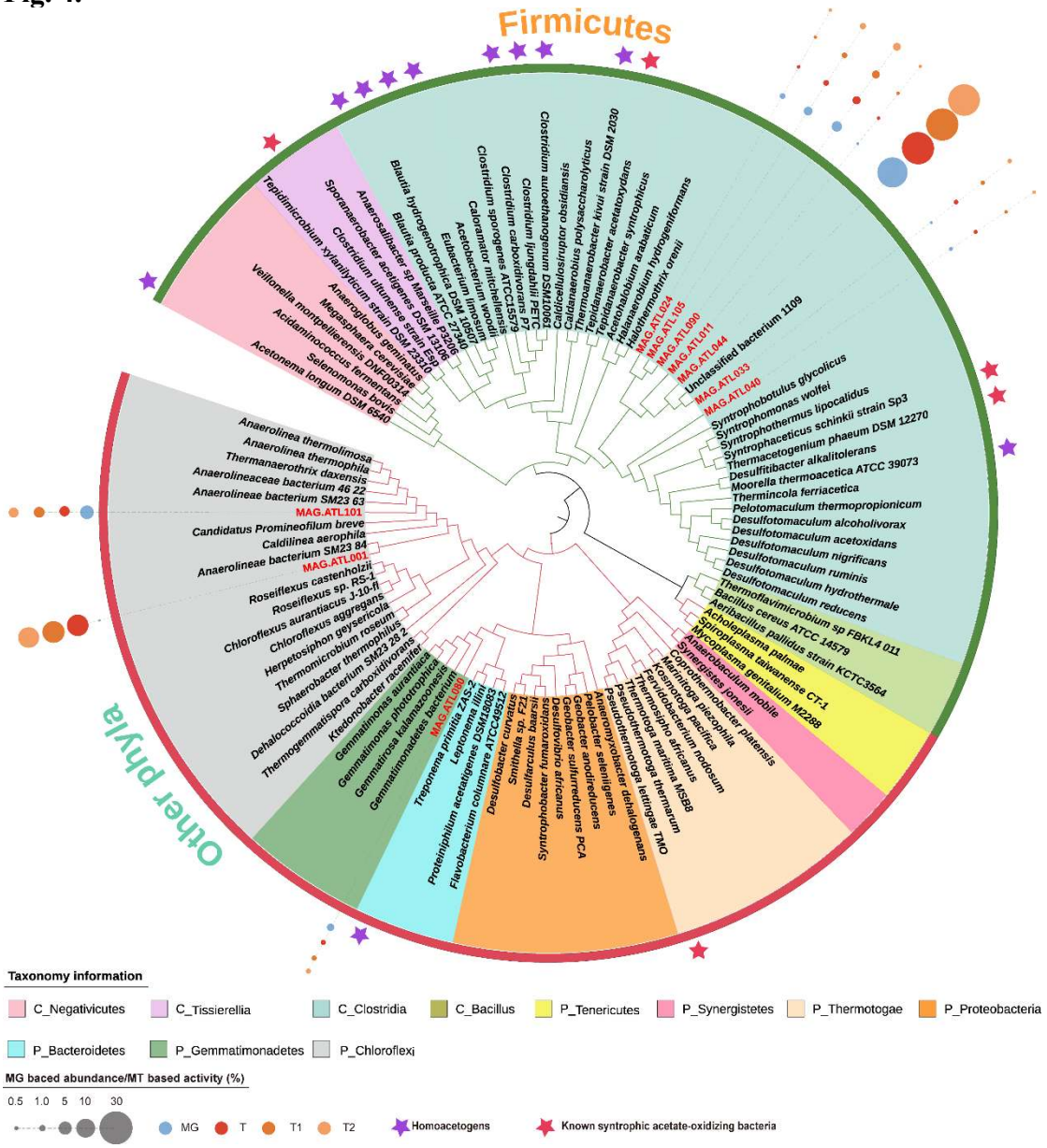

954

bioRxiv preprint doi: https://doi.org/10.1101/2021.07.06.451242; this version posted July 6, 2021. The copyright holder for this preprint (which was not certified by peer review) is the author/funder, who has granted bioRxiv a license to display the preprint in perpetuity. It is made available under aCC-BY-NC-ND 4.0 International license.

955 **Fig. 5**

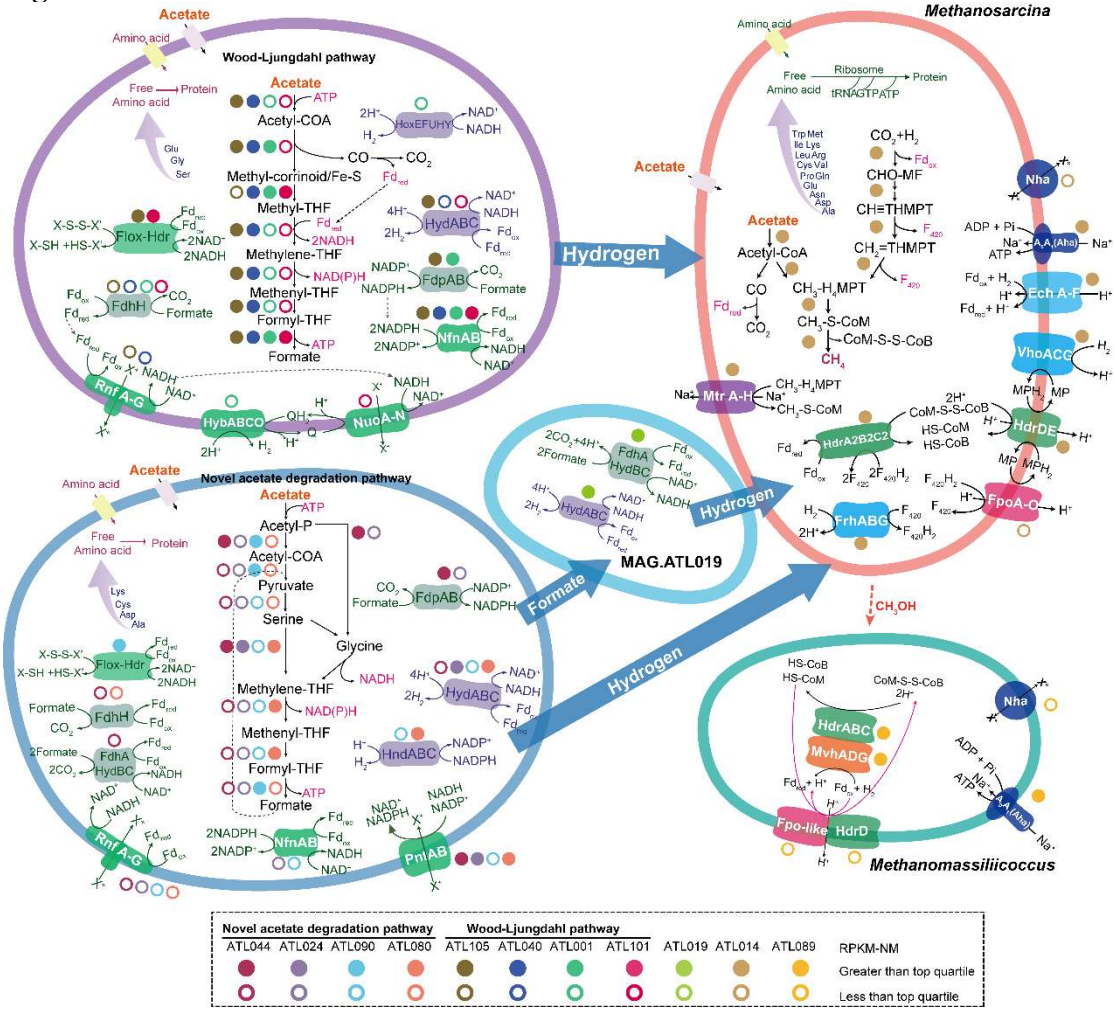

956

bioRxiv preprint doi: https://doi.org/10.1101/2021.07.06.451242; this version posted July 6, 2021. The copyright holder for this preprint (which was not certified by peer review) is the author/funder, who has granted bioRxiv a license to display the preprint in perpetuity. It is made available under aCC-BY-NC-ND 4.0 International license.

Fig. 6